

**MAPPING AND SAMPLING THE OCEAN FLOOR IN THE
HAYES FRACTURE ZONE AREA, MID-ATLANTIC RIDGE – THE
LUSO 2012 EXPEDITION (LEG 1), ON BOARD OF NRP
ALMIRANTE GAGO COUTINHO**

Pedro Lopes Ferreira



Aprovado para distribuição

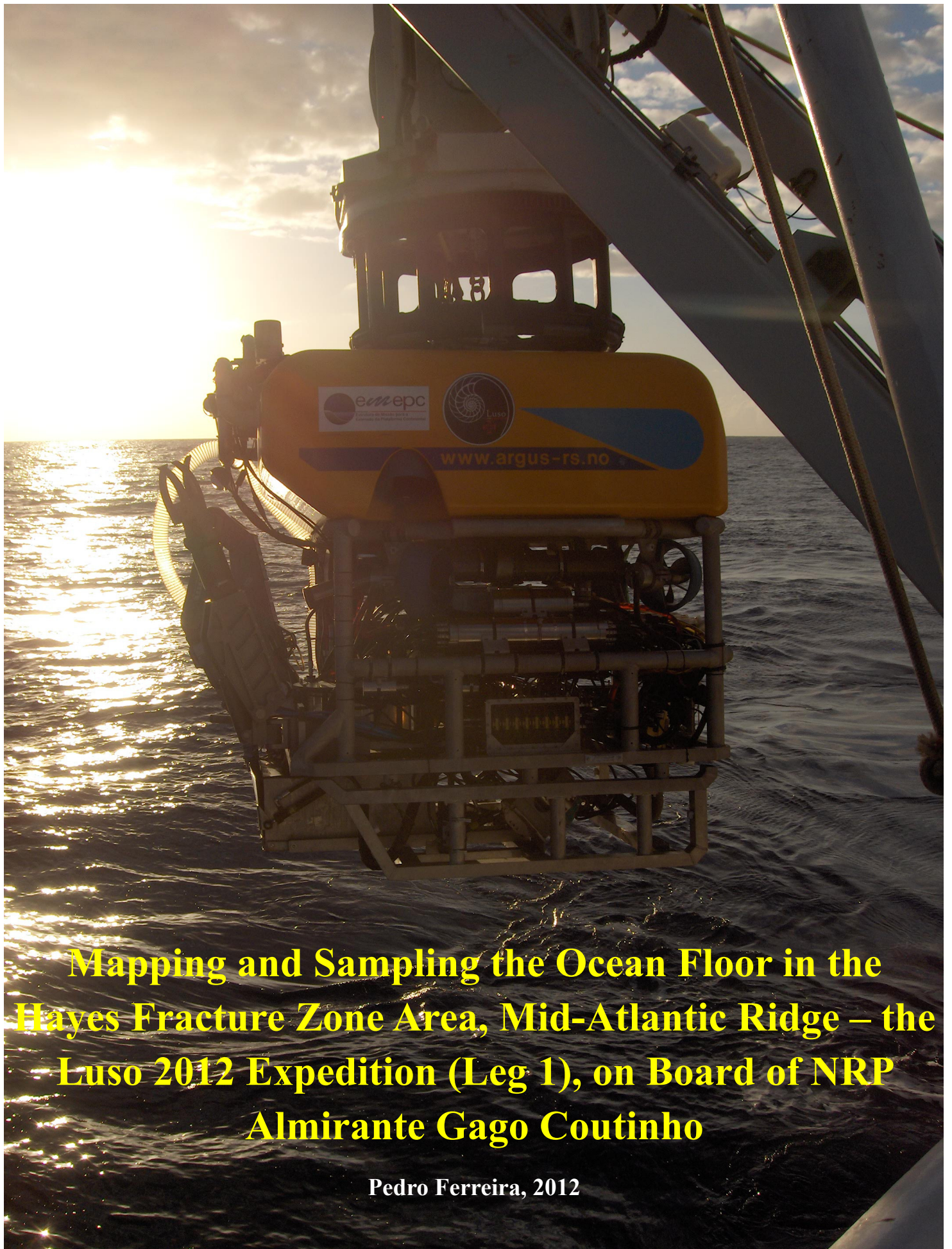
Data ___ / ___ / ____

O Interlocutor da

Unidade de Geologia Marinha

Unidade de Geologia Marinha
Estrada da Portela – Zambujal
Apartado 7586
2721-866 AMADORA





**Mapping and Sampling the Ocean Floor in the
Hayes Fracture Zone Area, Mid-Atlantic Ridge – the
Luso 2012 Expedition (Leg 1), on Board of NRP
Almirante Gago Coutinho**

Pedro Ferreira, 2012

LEG 1 – Hayes Fracture Zone area

1. Introduction

This leg started on 28th August, departing from Setubal and finished on the 20th September in Madeira Island. The calendar and arrival date of this leg were dramatically changed due to the formation of a hurricane in the North Atlantic (to which was given the name of Nadine), quite near from the planned working area for this leg. As a result, the NRP Gago Coutinho had to diverge the previously intended route (end of the leg in the Terceira island) directly to Madeira island to escape from the very strong winds and waves formed due to the hurricane. The table below gives a summary of the operations / transits made during this leg 1.

Date	Operations / Transits
28/08	Boarding at 09.00 and depart at 11.00 from Setubal harbor
28/08 – 02/09	Transit from Setubal to Terceira island (Azores). Tests with USVP's (Underway Sound Velocity profiler), dynamic with EMEPC equipment and static with the instruments of the Portuguese navy. Magnetic survey along the way. Arrival at 08.00 to Terceira island.
03/09 – 06/09	Tests with the ROV Luso in the vicinity of Terceira Island. Various operations of deployment and recovery of the ROV from and to the ship. Testing all the ROV instruments. A problem with a hydraulic pump was identified and a new one had to come from Lisbon. The tests finished with a dive reaching 2000 m depth in the Serreta area (L12D10). Departure to Hayes Fracture Zone area at 13.00.
07/09 – 09/09	Arrival in the morning to the studying area. Sturdy undulation and strong winds prevented the realization of any ROV dive. Bathymetry is done.
10/09	At 08.00 the ship stopped for the realization of the first ROV dive (L12D11). The area is located East of the Mid-Atlantic Ridge (MAR) and the depth is around 1500 mbsl. Strong current imply a slow descend of the ROV (2 hours and 30 minutes for the 1500 m). After 2 hours on the ocean bottom the ROV's sample container (that was open) was broken due to a collision with a basaltic outcrop. The container is lost and subsequently recovered and grabbed by the ROV's fix arm. The dive is suspended and the ROV return to the ship. During the ROV's ascent, the only sample collected during the survey is lost from the container. Already in the deck, the ROV presents

	one of the engines loose and is substituted. The sample container is fixed too. Due to these maintenance operations the dive predicted to the end of the afternoon is postponed.
11/09	First dive in the study area with successful rock sampling (L12D12). A sedimentary crust (limestone concretion) and some pillow lava fragments are recovered. The ROV was on the ocean bottom just for one and a half hour because two ROV's cameras stopped working.
12/09	Unfavorable wind and current conditions prevent the execution of any ROV dive.
13/09	ROV dive at South of the Hayes FZ and to the East of the MAR (L12D13). Fantastic dive finishing in the top of an haystack (submarine volcanic structure). Abundant lava tubes and pillows. ROV in the bottom for 3 hours and half.
14/09	Very strong wind in the morning. Ship moved to NE to allow a ROV dive at the end of the afternoon in a shallow area located E to OH-3 segment. The maintenance of the weather conditions prevents any ROV dive.
15/09	Same weather conditions (wind with 20-30 knots) and 3 meters waves. No ROV dives at all. Bathymetric and magnetic surveys.
16/09	Significant improvement in the weather conditions. However when everything is prepared for a ROV dive, a bad weather warning was received on the ship. The generation of a severe and well marked low- pressure to the West of our position was identified. This would evolved to the Hurricane that was given the name of Nadine. The first leg in the Hayes FZ area had to be interrupted and for security reasons we had to sail to Madeira island.
17/09 – 20/09	Transit to Madeira Island and arrival on the 20th September. End of Leg 1.

The Leg's participants to the Hayes Fracture Zone area were:

Scientific Team:

Pedro Madureira (Chief Scientist), EMEPC

Filipa Marques, EMEPC

Pedro Ferreira, LNEG

Diogo Geraldés, EMEPC

Pedro Mendes, Univ. Coimbra

ROV's Pilots / Technicians:

António Calado, EMEPC

Andreia Afonso, EMEPC

Miguel Souto, EMEPC

Bruno Lourenço, EMEPC

Renato Bettencourt, EMEPC

Jorgen Welde, Argus Remote Systems

Frank Widme, Argus Remote Systems

The main Leg 1 objectives were defined as follows:

- Collection of bathymetry data and rock samples in the north and south areas of the Hayes Fracture Zone;
- Characterization of the biodiversity in areas near the mid-Atlantic Ridge;
- Collection of magnetic data during transects sub-perpendicular and sub-parallel to the ridge axis;
- Collection of water samples from different depths (bottom, 600m, 200m) for microbiology studies;
- ROV and scientific equipment testing;
- ROV team training onsite.

2. The Mid-Atlantic Ridge in the Northern region between 33°N and the Azores

General Characteristics

Since 1991, the MAR has been extensively surveyed between 33°N and the Azores Archipelago. Many cruises were conducted in order to establish bathymetric maps, study the segmentation, look for hydrothermal anomalies in the water column or sample basalts, massive sulphides, hydrothermal fluids or biological material (e.g. Detrick *et al.*, 1995; Langmuir *et al.*, 1997; Charlou *et al.*, 2000, and references therein). The first bathymetric maps in this MAR

region were obtained using the EM12 system during the FARA-SIGMA cruise in 1991 (Needham *et al.*, 1992).

The MAR between 33° and 41°N exhibits a gradient in seafloor depth, from 3500 m just north of the Hayes Transform near 33°N to less than 1000 m near 39°N. Together with this depth gradient, the MAR is characterized by a broadening with a funnel shape best represented by the 2000 m bathymetric contour. This large bathymetric structure representing a volcanic topographic high is designated by Azores Platform (Fig. 1).

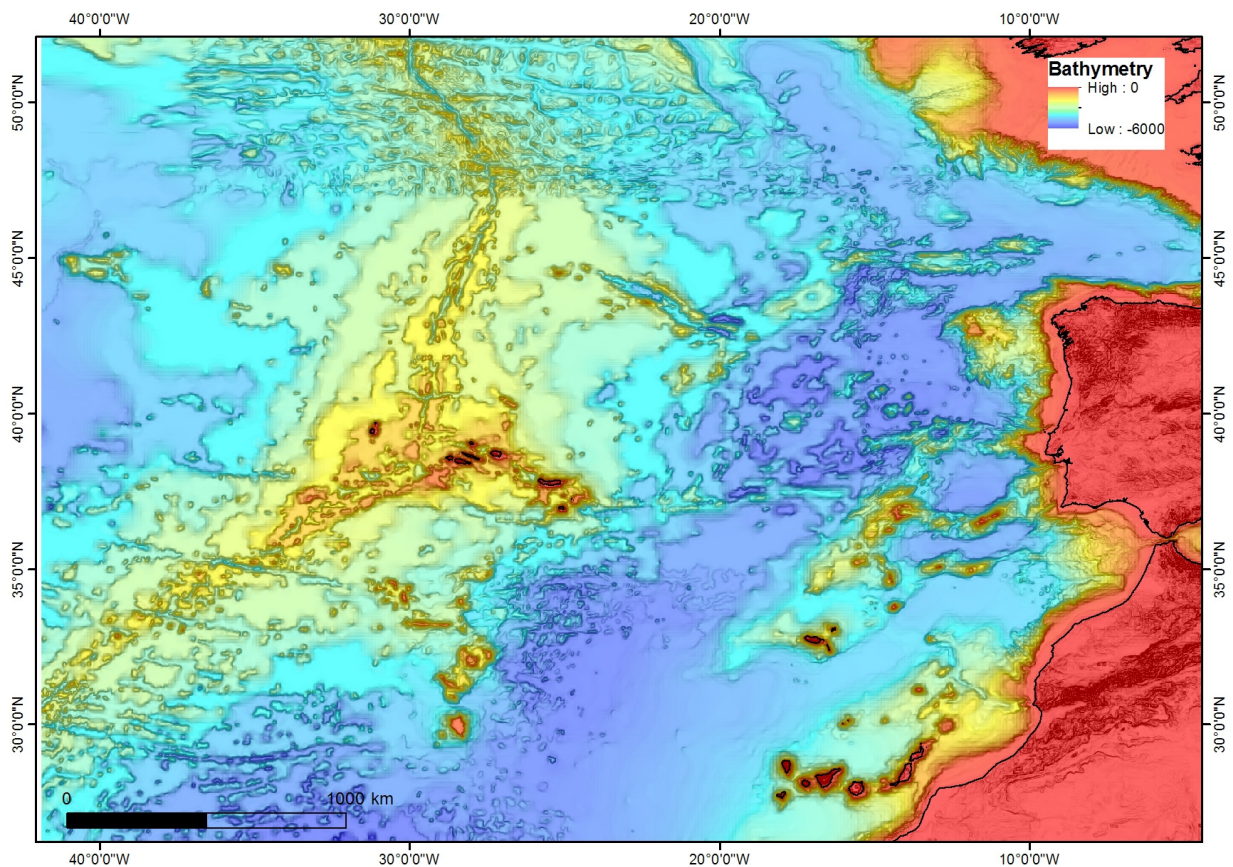


Fig. 1. Bathymetric map of the Mid-Atlantic Ridge (MAR) in the Azores region between 26°N and 52°N from satellite-derived bathymetry (Smith & Sandwell, 1997), emphasizing the existence of the Azores Platform.

The Azores platform presents a high tectonic complexity due to the existence of a triple junction between the American, Euroasian and African Plates. The boundary between the Eurasian and African plates has always been contentious but, presently, is considered as represented by the NW-SE lineament of São Miguel-Terceira-Graciosa (Terceira rift) (Fig. 2) and several models

have been proposed to describe the plate kinematics along this boundary: pure extension, pure strike-slip and a combination of both (e.g. Krause & Watkins, 1970; Searl, 1980; Madeira & Ribeiro, 1990; Lourenço *et al.*, 1998).

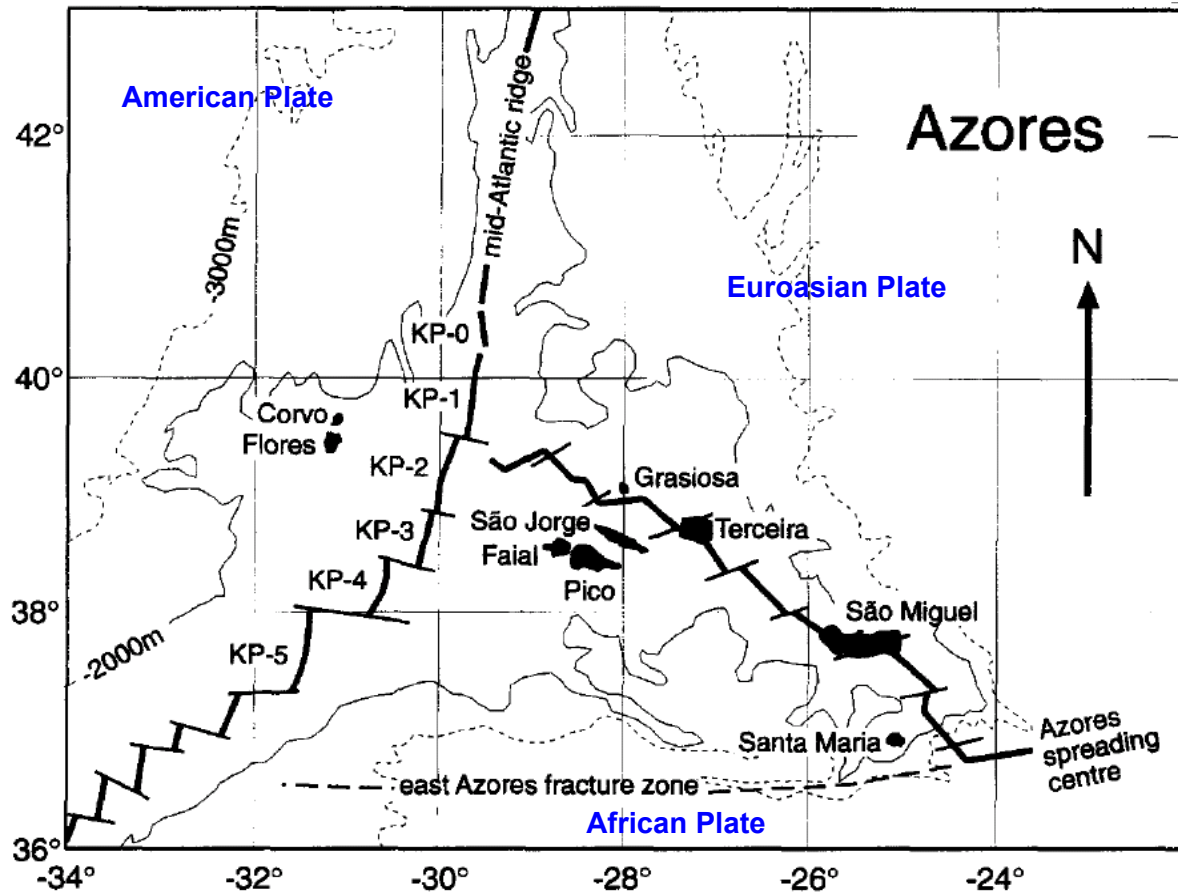


Fig. 2. Map of Mid-Atlantic Ridge – Azores Platform region showing the locations of the Azores volcanic islands, simplified bathymetry and the synthetic geodynamic setting (adapted from Turner *et al.*, 1997). The islands, except Corvo and Flores (belonging to the American plate), are located between the so called Terceira rift (joining São Miguel, Graciosa and Terceira islands) and the East Azores Fracture Zone.

The maximum bathymetric expression of this platform is given by the emergence of a group of nine volcanic islands, forming the Azores archipelago. Seven islands (Santa Maria, São Miguel, Terceira, São Jorge, Graciosa, Pico, and Faial) stand at the East of the ridge (Eurasian plate) whereas the other two (Corvo and Flores) are located to the West of MAR, on the North American plate (Fig. 2). The islands form a broad WNW-ESE lineament between 31°W and 24 ° W longitude, that crosses the MAR at a latitude of ~ 39°N, in the KP-2 segment.

The importance of the formation of the Azores Platform was firstly raised by Schilling (1975) that ascribed its generation to plume activity based on the fact that tholeiitic basalts from the MAR along the Azores Platform exhibit a greater degree of LREE enrichment than tholeiites from normal ridge segments, and that there is a progressive increase in LREE enrichment as the platform is approached (Schilling, 1975). The platform tholeiites have been known to have correspondingly high concentrations of large-ion-lithophile elements (LILE) and high $^{87}\text{Sr}/^{86}\text{Sr}$ ratios (White *et al.*, 1976; White & Schilling, 1978) as well as high Pb and low Nd isotopic ratios (Dupré & Allègre, 1980; Dupré *et al.*, 1982; Ito *et al.*, 1987; Yu *et al.*, 1997; Dosso *et al.*, 1999). This geochemical enrichment was found to correlate with a topography high and a negative gravity anomaly, which were suggestive of mantle upwelling beneath the Azores, and consistent with a hotspot origin (Schilling, 1975).

The Azores hotspot corresponds to a broad (a few hundred kilometres in diameter) domain of anomalously low S-wave velocities in the 100 km to 200 km depth range, centred somewhat to the east of the MAR (Zhang & Tanimoto, 1992). The distribution of recent volcanism in the Azores archipelago suggests a similar location (100 to 200 km to the east of the ridge, near the island of Faial) for the hotspot centre (Schilling, 1985; Ito & Lin, 1995). However, the size, depth and the accurate location of this mantle anomaly are still a matter of debate.

Besides being characterized by a topographic high, the Azores platform has a crustal thickness 60% higher than normal, according to the seismic refraction studies (Searl, 1980) as well as detailed modelling of the gravity field (Detrick *et al.*, 1995). The morphology is also anomalous in the shallowest zones of the MAR platform where the axial valley is less marked and the segments are swollen (e.g. Detrick *et al.*, 1995). This situation is also present in the Reykjanes ridge by the segments closer to Iceland (e.g. Parson *et al.*, 1993). These anomalies are also visible in large-scale gravity maps (Cochran & Talwani, 1978) with residual gravity anomalies as high as ~ 30 mgal on the Azores platform (Fig. 3). Modelling of these features has shown that they can be explained by a large mass of anomalously hot mantle (about 75°C above normal) located at a depth of a few hundred kilometres (Cochran & Talwani, 1978). Through the geophysical anomalies modelling, Sleep (1990) has estimated a buoyancy flux of 1.1 Mg s^{-1} for Azores hotspot.

The MAR in this region is segmented by four large discontinuities: Kurchatov ($\sim 40^\circ\text{N}$), the Pico ($\sim 38^\circ\text{N}$), the Oceanographer ($\sim 35^\circ\text{N}$), and the Hayes ($\sim 33.5^\circ\text{N}$) fracture zones, which

delineate three main ridge sections (Fig. 4). The Pico – Kurchatov section has a length of ~ 325 km and six second-order segments, referred to as KP-0 to KP-5, have been documented (Detrick *et al.*, 1995; Goslin, 1999). The Pico to Oceanographer (PO) section is about 275 km long, and composed of eight second-order segments, referred to as PO1-PO8. Lastly, the Oceanographer to Hayes (OH) section is formed by five second-order segments (OH-1 to OH-5) and extends for about 220 km long. These segments have lengths between 10 and 100 km and are linked by a series of systematic left-lateral, non-transform offsets (NTOs; e.g. Parson *et al.*, 2000). The NTOs are broad areas where a gradual transition between adjacent spreading segments involves no significant transform faulting. They are defined as spatial offsets of 15 km to 30 km and age offsets of 1-3 Ma and have small segment length / offset ratio (e.g. Grindlay *et al.*, 1991; Sempéré *et al.*, 1993; Gràcia *et al.*, 2000).

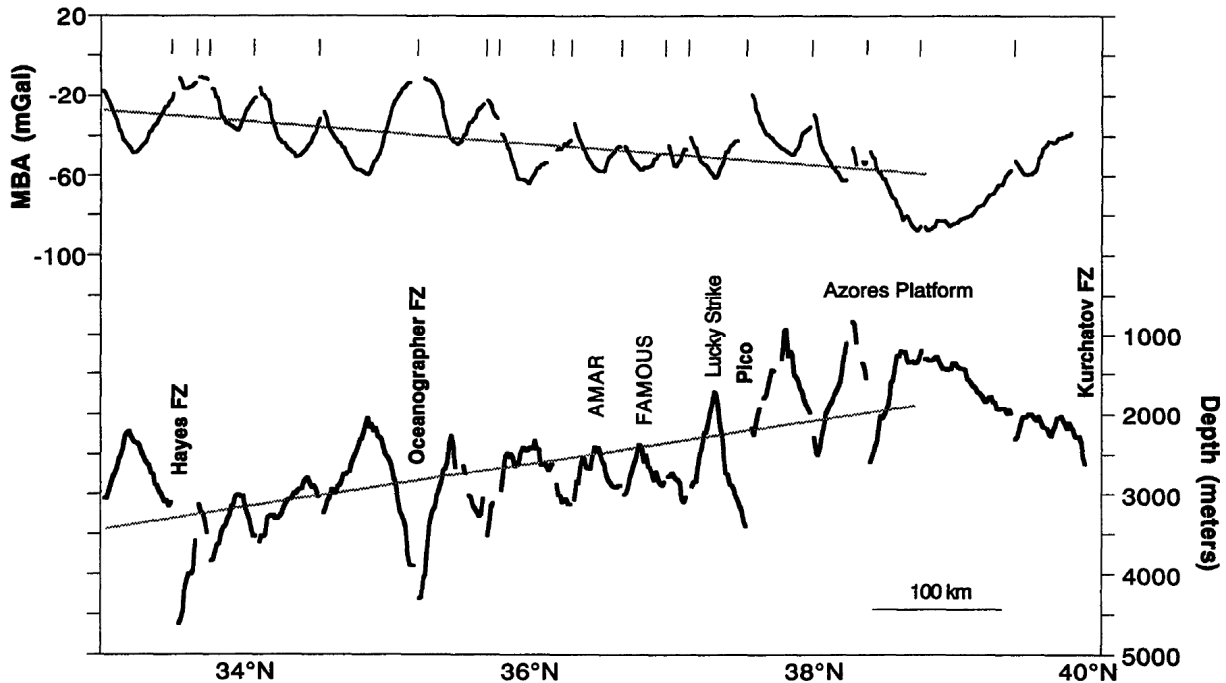


Fig. 3. Variation in axial depth (bottom irregular line) and mantle Bouguer anomaly (MBA) (top irregular line) along the MAR axis between 33°N and 40°N (adapted from Detrick *et al.*, 1995). The two straight lines represent the best fit to the data and illustrate the longer wavelength gradient in depth and gravity away from the Azores. Short vertical bars represent the locations of segment offsets. Note that the shorter wavelength corresponding to the segment-scale variation is also observed. MBA lows are associated with shallow axial depths and are located near segment midpoints. Conversely, MBA highs and depth maxima are observed near segment offsets.

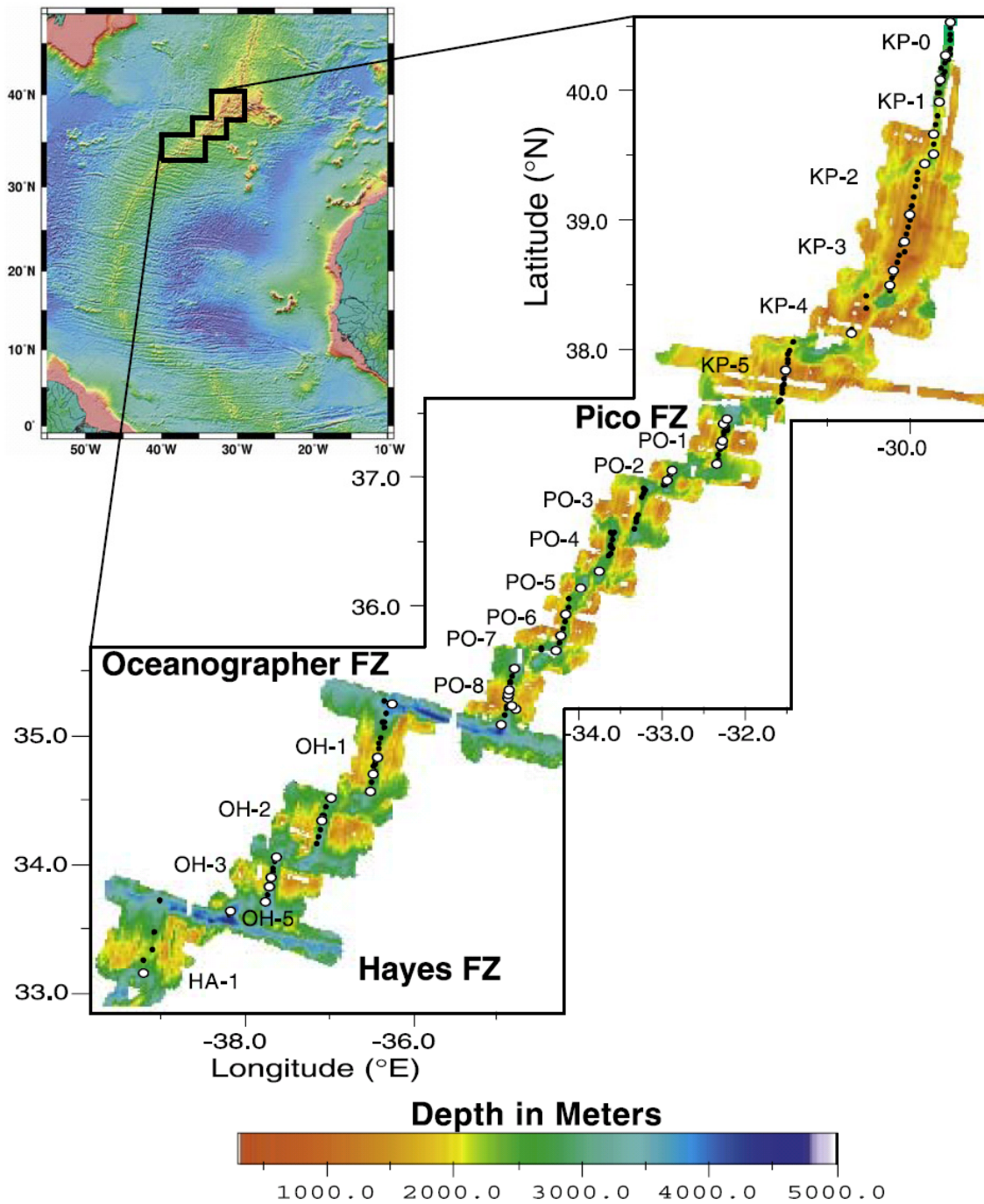


Fig. 4. Localization and nomenclature of the segments along the MAR between 33°N and 40.5°N (adapted from Asimow et al., 2004). Pico, Oceanographer and Hayes fracture zones referred to by their common names are also shown. Simplified bathymetry of the MAR section based on data from SIGMA cruise (Detrick et al., 1995; Bougault et al., 1997). Black and white dots represent sample locations where glass was recovered from the FAZAR cruise. Inset is shaded relief image of satellite-based bathymetry of Smith & Sandwell (1997).

The NTOs at the MAR south of Azores are characterized by the presence of shallow, dome-like shaped massifs, oblique to parallel to the ridge, with complex structural fabrics accommodating the offset. Some of these massifs have been explored and sampled, revealing that they are composed of upper mantle peridotites and lower crustal rocks, and sometimes associated with high-temperature hydrothermal venting. The exposure of the ultramafic massifs within the NTOs is favoured by low magmatic supply and low-angle detachment faulting occurring at segment ends.

Side-scan sonar imagery along the MAR in Azores region allows detecting that sediment cover is marked by very distinct maxima, mainly restricted to the non-transform discontinuities and the volcanic processes are mainly confined to the segments interior (e.g. Blondel, 1996; Parson *et al.*, 2000). Neo-volcanic activity declines with distance from the Azores, which is consistent with previous observations (e.g. Detrick *et al.*, 1995; German *et al.*, 1996; Parson *et al.*, 2000). In contrast, tectonic activity increases with distance away from the hotspot, but is not restricted to spreading segments. The northern segments are more affected by volcanism and the southern segments by tectonics. This is explained by the declining influence of the Azores hotspot with distance (Blondel, 1996; German *et al.*, 1996).

Several active sites of hydrothermal venting have been found and sampled on the MAR in the Azores region including from north to south, “Menez Gwen” (Fouquet *et al.*, 1994, 1995; Ondréas *et al.*, 1997), “Lucky Strike” (Langmuir *et al.*, 1993, 1997; Fouquet *et al.*, 1994, 1995; Humphries *et al.*, 2002), “Rainbow” (German *et al.*, 1996) and “Saldanha” (Bougault *et al.*, 1997; Barriga *et al.*, 1998). Whereas the first two hydrothermal fields are located at the central topographic highs of the corresponding segments and are developed within a basaltic crustal substratum, the remaining two are related to high-temperature interaction between seawater and serpentinized ultramafic rocks from the upper mantle, outcropping in the NTOs: “Saldanha” is located at the east end of the FAMOUS/AMAR NTO (PO-3/PO-4) and “Rainbow” is located in the NTO between AMAR / South AMAR (PO-4/PO-5). The circulation of hydrothermal fluids and the occurrence of high-temperature vent sites associated with NTOs are probably favoured by the pervasive fracturing and faulting at these discontinuities (Gràcia *et al.*, 2000) (Fig. 5).

The MAR spreading rate increases from South (35°N) to North (40°N) from 20 to 22 mm/yr (DeMets *et al.*, 1990) and has been almost constant since 40 Ma (Cande *et al.*, 1985).

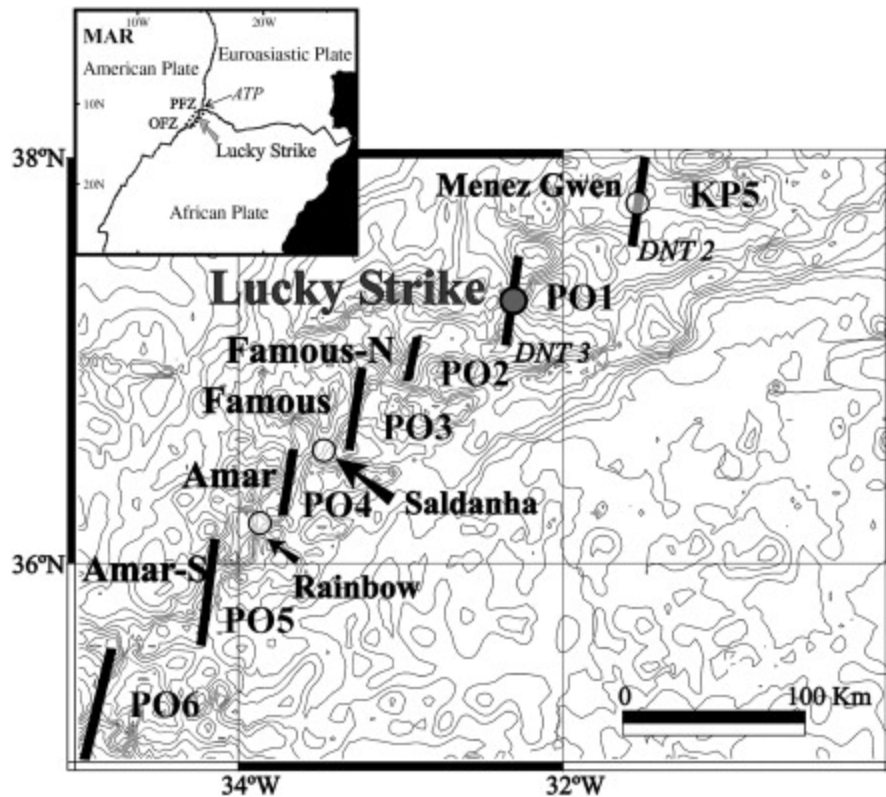


Fig. 5. Area between the Pico Fracture Zone (PFZ) and the Oceanographer Fracture Zone (OFZ) along the Mid-Atlantic Ridge (MAR), south of the Azores Triple Point (ATZ) showing the location of the existent Hydrothermal fields.

Geochemistry

It is well known that mid-ocean ridge basalts (MORB) are dominated by incompatible-element depleted normal tholeiite (N-MORB). However, the identification of less depleted, and even incompatible-element enriched basalts (E-MORB), resembling those from ocean islands, is becoming more frequent with the increasing number of mid-ocean ridge segments sampled. These observations suggest that the upper mantle beneath ocean ridges is heterogeneous. This mantle heterogeneity is apparent when analyzing the isotopic composition of MORB lavas from spreading ridges in the three major ocean basins (Fig. 6). Figure 6 shows that, besides a significant range of the various Sr-Nd-Pb isotopic ratios present in a single ocean basin, there are systematic isotopic differences between MORB from different ocean basins. This diversity reflects some very large scale isotopic heterogeneities in the mantle source of these basalts. Thus, although the unequivocal evidence for the existence of a geochemically heterogeneous

Earth's mantle, the origin, size, and history of the enriched heterogeneities in the dominantly N-MORB mantle generally remain enigmatic.

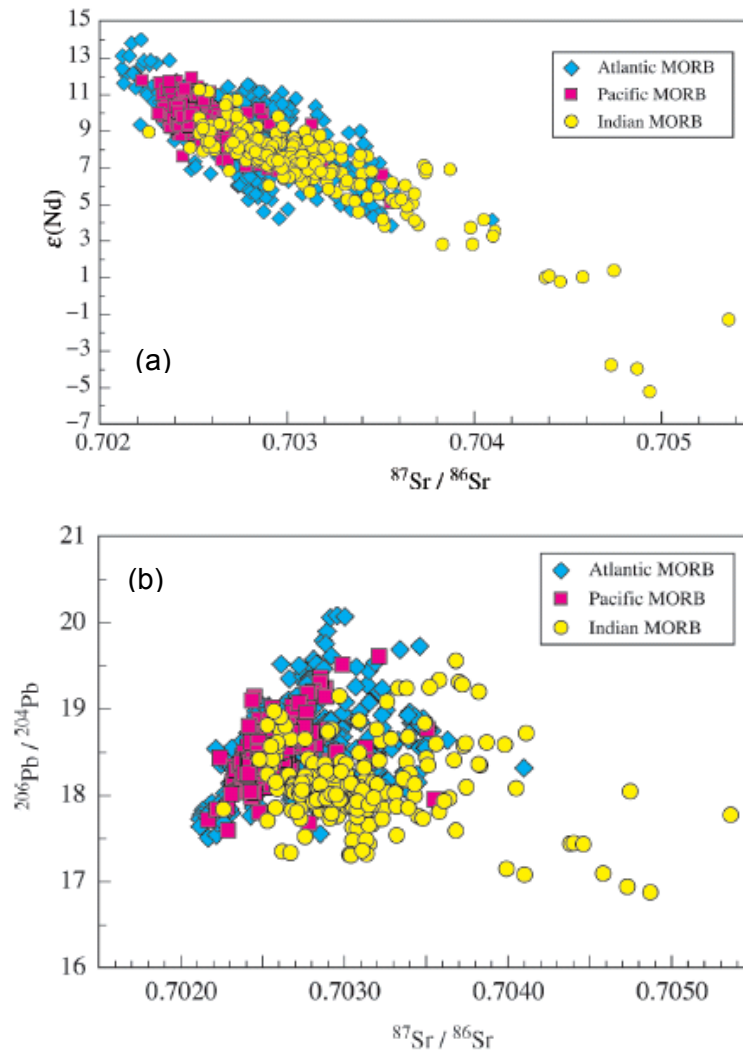


Fig.6. $^{87}\text{Sr}/^{86}\text{Sr}$ vs. $\epsilon(\text{Nd})$ and (b) $^{206}\text{Pb}/^{204}\text{Pb}$ vs. $^{87}\text{Sr}/^{86}\text{Sr}$ for MORB from three major ocean basins. Adapted from Hoffman (2003).

The origin of mantle heterogeneities along the MOR system fall into two general causes: a) those where the ridge is located away from any hotspot and, consequently, is not affected by the hot-spot type magmatism derived from such mantle structures; b) those where the ridge is being influenced by a hotspot and produces lavas enriched in incompatible elements and showing elevated Sr-Nd-Pb radiogenic values (Fig. 7).

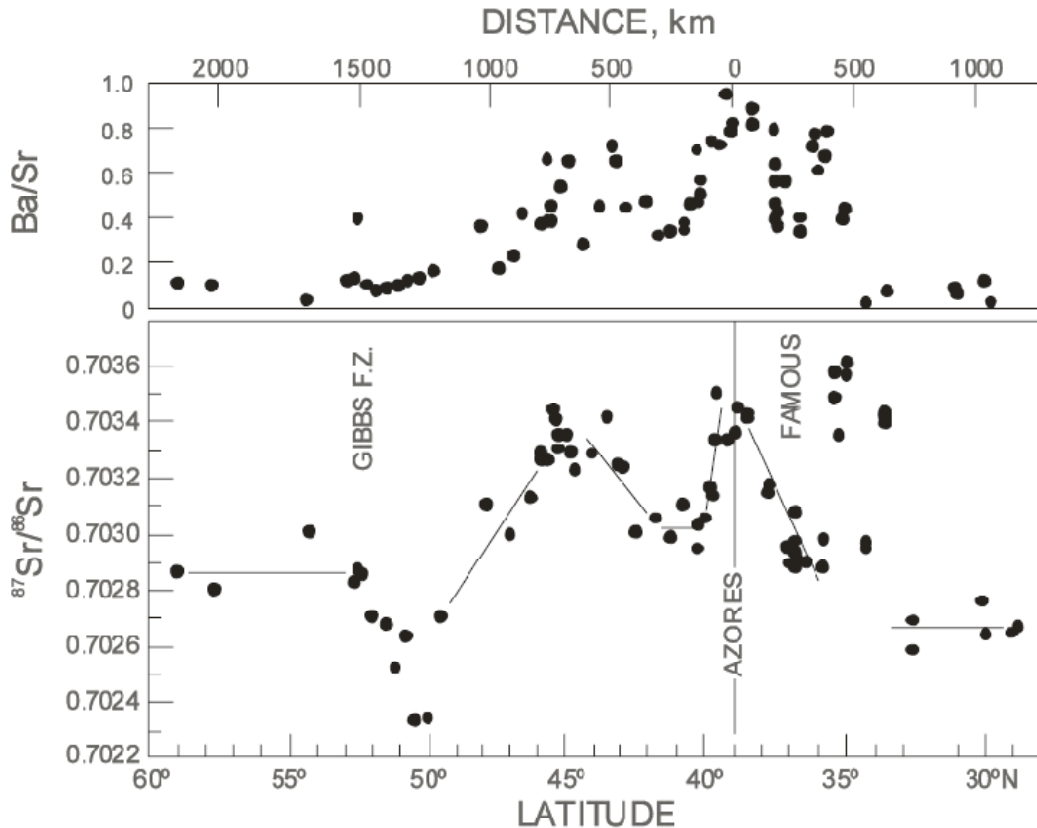


Fig.7. Variation of Ba/Sr and ⁸⁷Sr/⁸⁶Sr ratios along the MAR between ~ 30°N and 60°N as a result of MAR – Azores hotspot interaction (adapted from White & Schilling, 1978).

Distinct trace element relationships presented by lavas collected along a designated MOR section could indicate the existence of a certain degree of mantle heterogeneity in their mantle source(s). However, since trace element ratios are affected by different melting regimes, as well as by the extent of partial melting, further evidence is needed to distinguish these mantle processes. Normally, this is given by several radiogenic isotopic ratios. Lavas having different values for these ratios indicate that they originated from distinct mantle sources. The sampling of incompatible element enriched lavas, having simultaneously more radiogenic isotope values, away from any known hotspot, has been described (e.g. Michael *et al.*, 1994; Niu *et al.*, 1999; Donnelly *et al.*, 2004). Such heterogeneities may consist of more fertile mantle portions that are passively embedded in the ambient depleted upper mantle. These fertile domains would have the opportunity to segregate more enriched melts in comparison to those derived from the depleted upper mantle. It seems reasonable to attribute the origin of such heterogeneities to the continuing oceanic lithosphere subduction into the mantle, because this process has been

contributing throughout geological time to the geochemical evolution of the earth's mantle. It can be envisaged that a certain amount of this recycled material could mix with the depleted upper asthenosphere and produce individual mantle domains more enriched in incompatible elements and radiogenic isotopes. If these domains were delivered to a region beneath the MOR system, by mantle convection, the subsequent adiabatically uprising mantle will generate such E-MORB lavas. Alternatively, less depleted portions of lower mantle reservoirs might be involved, entrained in the upper mantle by processes not associated with mantle plumes.

In the case of a ridge section under the influence of a mantle plume, the enriched character of the MORB lavas is directly linked to the plume mantle material. Mantle plumes are thought to represent buoyant material that separates from a thermal and, probably, compositional boundary layer either at the base of the mantle or at the 660-km boundary and typically develops a head and tail structure as it ascends through the mantle (e.g. White & McKenzie, 1989; Davies, 1999). The remaining tail structure of these plume-like thermal anomalies was considered to be near-cylindrical in shape (e.g. Campbell & Griffiths, 1990). The general character of the plume model is supported by seismic tomography, which has allowed direct imaging of plumes rising from both mid-mantle and deep-mantle depths (e.g. Nataf, 2000; Zhao, 2001). However, contrasting results indicating the plumes existence as being ambiguous or precluding the possibility of deep-rooted origin for these anomalies have also been published (e.g. Anderson *et al.*, 1992; Ritsema & Allen, 2003).

A further association allowed by the plume model is the mixing of MORB-source with lower mantle material derived from the plume (e.g. Galer & O'Nions, 1985; Sun & McDonough, 1989). Lateral flow of plume material and, consequently, its entrainment in the neighbouring asthenospheric reservoir, will produce mixing relationships along the ridge, which should show an increasing plume character with decreasing distance to the hotspot (Schilling, 1975).

The size of mantle heterogeneities, can be assessed directly from the study of mantle rocks constituting ultramafic xenoliths that are included in alkaline volcanic rocks and kimberlites. Further equivalent information can be obtained by studying the chemical variability in high-temperature orogenic lherzolite massifs exposed on land. These remarks, at small spatial scales, coupled with those derived by the isotopic variation found in oceanic lavas at a global-scale, indicate that mantle heterogeneities span a large range of scales (from cms to thousands km).

The northern Mid-Atlantic Ridge (MAR), between 31°N and the Azores archipelago (~ 40°N), comprises a significant ridge section (~ 1000 km long) in which lavas more enriched than the N-MORB are extruded (Fig. 7). Evidence for this enrichment was first presented by Schilling (1975) using REE geochemistry. Based on chondrite-normalized La/Sm ratios, the MAR was separated into three regions: one, south of 32°N, having low and relatively constant ratio values (<1), typical of N-MORB; the second, corresponding to a transition zone, between 34°N and the Azores platform (38°N), characterized by a constant increase in $(La/Sm)_{cn}$; the third, the MAR region that crosses the Azores platform, having the highest $(La/Sm)_{cn}$ ratio. This geochemical trend was corroborated during subsequent years, through research on other samples spatially distributed along the MAR in this region, by reporting of other incompatible element ratios (White & Schilling, 1978; Bougault & Treuil, 1980; Schilling *et al.*, 1983) and Sr isotopic ratios (White *et al.*, 1976).

Coupled to the geochemical gradients there are often systematic variations in bathymetry, for example the MAR shoals by several thousand meters from 33°N to the Azores archipelago (e.g. Ridley *et al.*, 1974; Detrick *et al.*, 1995). Associated with this bathymetric anomaly, a regional, long-wavelength, gradient away from the Azores characterizes the mantle Bouguer anomaly (Fig. 3). Gravity-derived crustal thickness (e.g. Cochran & Talwani, 1978) together with seismic refraction data obtained along the MAR in the Azores region (e.g. Searl, 1980) have showed a gradual increase in the average crustal thickness with proximity to the Azores, suggesting an increase in melt supply. The resulting overall crustal thickening from 33°N toward Azores archipelago region was estimated to be ~ 3.5 – 4 km.

Combining the geochemical evidence, with the geomorphologic and geophysical characteristics for this region, Schilling (1975) suggested the existence of a mantle plume beneath the Azores platform, as an analog to the interpretation proposed by Morgan (1971) for the Iceland region. Implied in this theory was the existence of two distinct mantle sources – one, impoverished in incompatible elements, which generates the typical N-MORB, and the other enriched in these elements, both separated in space but connected by a mixed transition region involving magmas derived from these two reservoirs. The so-called Azores Platform, which is located between 37° and 40°N, contains the nine Azores islands, is characterized by a funnel-shaped bathymetric swell. The widest lateral extent of this swell is located at the MAR – Azores islands intersection. Both the Azores platform and its island group represent the maximum expression of the hotspot effect on the oceanic crust in this region.

More recently, intensive rock sampling was conducted during the FAZAR expedition along the neovolcanic zone of the MAR from 33° 10', south of the Hayes transform fault, to 40° 30', just south of the Kurchatov transform (13 segments), where 213 sampling stations were performed. For comparison, the previously large scale sampling campaign for this region had collected one or two dredges from most segments. It was this new sampling that allowed Schilling (e.g. 1975) to define the long geochemical wavelength gradient towards the Azores platform. When integrating the new chemical (trace elements and Sr-Nd-Pb isotope data) and geophysical data obtained during this expedition, the geochemical, bathymetric and gravimetric gradients south of the Azores were confirmed (Detrick *et al.*, 1995; Dosso *et al.*, 1999). Hence, it appears that the northern Mid-Atlantic Ridge (MAR) between 31°N and 41°N is the site of a long wavelength geochemical anomaly associated with the Azores hot spot. This anomaly is established by a gradient in incompatible element concentrations, coupled with higher ratios in the more-to-less incompatible element ratios and more elevated radiogenic Sr-Nd-Pb values, all increasing towards the Azores archipelago.

The more exhaustive rock sampling along the MAR during the FAZAR expedition added further information about the characteristics of the geochemical and geophysical gradients across the Azores region. One of the main geochemical outcomes was the evidence that some ridge segments have produced lavas that present a higher degree of enrichment in incompatible elements than the expected from the regional variation alone. Moreover, this local enrichment is also recognized in the Sr-Nd-Pb isotopic signatures. When plotting these geochemical parameters against latitude, the elemental enrichment produces local peaks that are detached from the regional trend (Dosso *et al.*, 1999).

This systematic geochemical variation at segment scales is even more striking when considering the bathymetric and the gravity data of Detrick *et al.* (1995) obtained in the same expedition (Fig. 3). Residual Mantle Bouguer Anomalies (RMBA), which result from correcting the free-air anomalies by the gravity effects of the seafloor topography and relief of the crust – mantle boundary, have typically low values in the segment midpoints (also called “bull’s eyes” anomalies) while segment ends are usually characterized by RMBA highs, supporting the previous results of Lin *et al.* (1990). This segment-scale variation in gravity has been ascribed primarily to along-axis crustal thicknesses differences of > 2-3 km between the middle and ends of spreading segments (e.g. Lin *et al.*, 1990; Detrick *et al.*, 1995). The agreement between the gravity-inferred crustal thickness variation and estimates made by seismic refraction over the

MAR (e.g. Sinha & Lowden (1983) and Detrick *et al.* (1995) for the region between the OH-1 and OH-3 segments) provides additional and independent evidence that the gravity signal variation is related to crustal thickness differences. These inferences are confirmed by the outcropping of peridotites at or near numerous segment ends and their off-set discontinuities, suggesting thin crust (e.g. Gracia *et al.*, 2000).

Niu *et al.* (2001) has undoubtedly associated these two types of data (geophysical and geochemistry) in the northern MAR, showing that the basalts most enriched in incompatible elements are located in the OH-1 and OH-3 segment centres, that constitute the shallowest portions of the entire segments. Moreover, these segment midpoints are also associated with the lowest RMBA values found along the corresponding segments. A generalization of this geochemical and geophysical data coupling is made by Langmuir *et al.* (1996) for most segments in the MAR under the influence of the Azores hotspot, but without the support of any published chemical data.

3. Results: Dives, observations and sample descriptions

North of Hayes Fracture Zone

The main objective for this area was the collection of bathymetry and basaltic rock samples. The area is included in the extended continental shelf, which was partially defined by the geochemistry of erupted lavas. Rocks sampled on the Azores platform are characterized by a specific trace element and isotopic signature that extends to the Hayes Fracture Zone. Most samples from public databases were collected in the rift valley and we tried to expand the knowledge on lava's composition to off-axis sites. The dives north of the Hayes Fracture Zone were all performed in the eastern side of the mid-Atlantic ridge at similar latitudes. The latter includes the higher reliefs in the area, which are also related with the center of the ridge segment, named OH3 by Bideau *et al.* (1996) and Gracia *et al.* (2000). These authors describe the presence of ultramafic core complexes and several basaltic units in the OH3 segment. The multibeam survey allowed the collection of bathymetric data of almost all OH3 segment (Fig.8). ROV operations showed that the most suitable areas to collect rock samples are those closer to the rift valley. Conversely, macrofaunal biodiversity (red corals, sponges, etc) appears to be

more important in relatively distal areas. Samples of basaltic pillows were only collected from one site that can be proximal to a hydrothermal vent area (suggested by the presence of a plume detected at 800 m deep during the ROV descent to the bottom at a depth of 1100 m). The collected samples are strongly porphyritic dominated by mm to cm plagioclase phenocrysts.

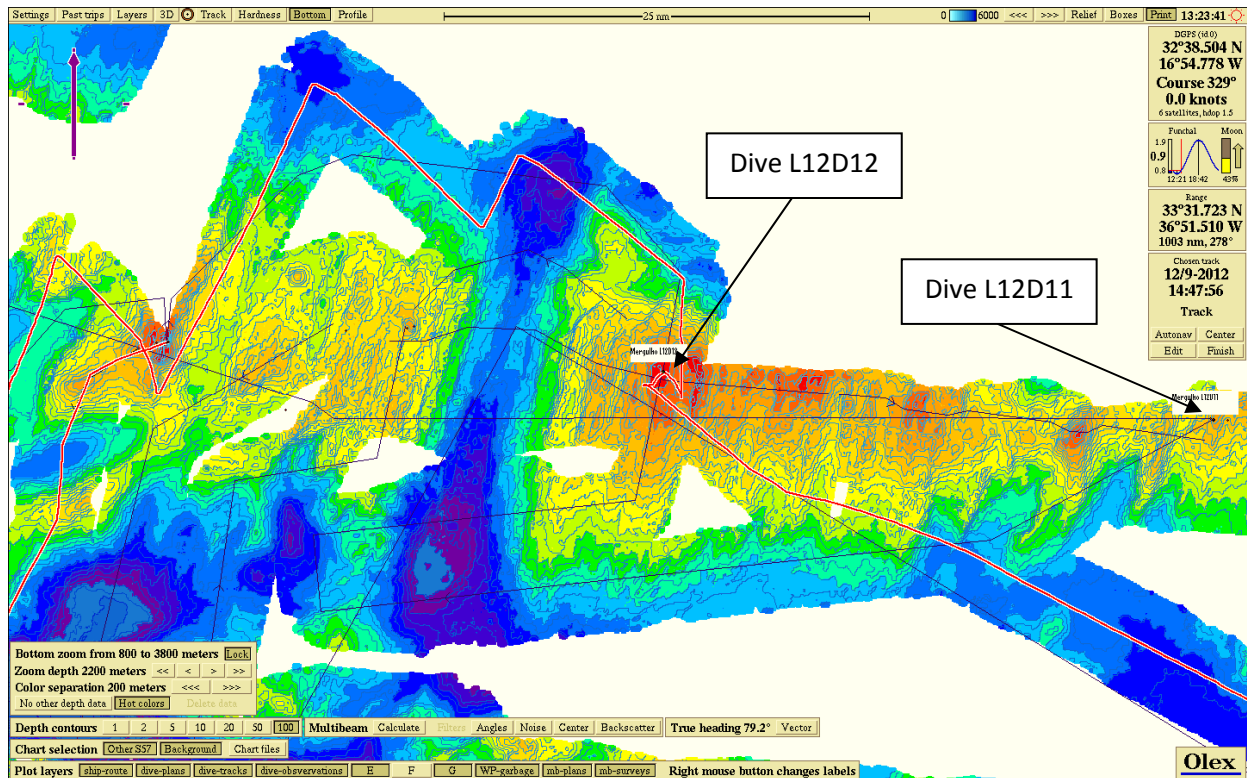


Fig. 8. Bathymetric chart of the area north to the Hayes Fracture Zone with the location of the ROV dives.

South of Hayes Fracture Zone

Again, the main objective for this area was the collection of basaltic rock samples. Basaltic samples from pillow lavas were recovered during one dive in the eastern flank of a small ridge segment (Fig. 9). The dive started at the base of a pillow mound, which was surveyed towards the top. The main feature of the sampled lavas is their aphanitic texture.

Details of the performed dives, collected samples and geological observations are presented in the following pages of this report, after the cited references.

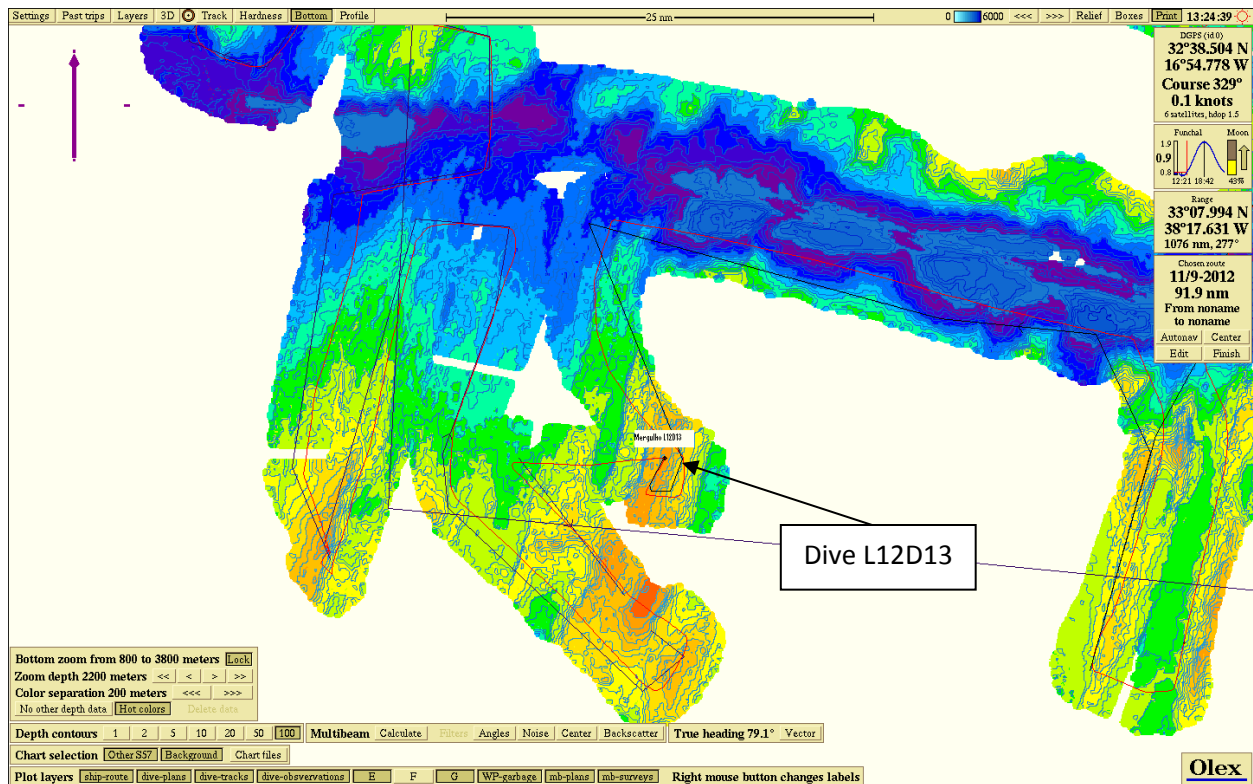


Fig. 9. Bathymetric chart of the area south to the Hayes Fracture Zone with the location of the ROV dives.

References

- Anderson, D.L., Tanimoto, T. & Zhang, Y. (1992). Plate tectonics and hot spots. The third dimension. *Science* **256**, 1645–1651.
- Asimow, P.D., Dixon, J.E. & Langmuir, C.H. (2004). A hydrous melting and fractionation model for midocean ridge basalts: application to the Mid-Atlantic Ridge near the Azores. *Geochemistry, Geophysics, Geosystems* **5**, doi: 10.1029/2003GC000568.
- Barriga F.J.A.S., Fouquet, Y., Almeida, A., Biscoito, M., Charlou, J.-L., Costa, R.L.P., Dias, A., Marques, A.M.S.F., Miranda, J.M.A., Olu, K., Porteiro, F. & Queiroz, P.S. (1998). Discovery of the Saldanha Hydrothermal Field on the FAMOUS Segment of the MAR (36° 30' N). AGU Fall Meeting 1998.
- Blondel, Ph (1996). Segmentation of the Mid-Atlantic Ridge south of the Azores, based on acoustic classification of TOBI data, in: MacLeod C.J. et al. (Eds.), Tectonic, Magmatic, Hydrothermal and Biological Segmentation of Mid-Ocean Ridge, *Geological Society Special Publication* **118**, 17-28.
- Bougault, H. & Treuil, M. (1980). Mid-Atlantic Ridge zero-age geochemical variations between Azores and 22°N. *Nature* **286**, 209–212.
- Bougault, H. et al., MARFLUX/ATJ – Mid-Atlantic Ridge: hydrothermal fluxes at the Azores Triple Junction, *MAST Final Report, Contract MAS2-CT930070, Open File Document*, IFREMER, Brest, 1997.
- Campbell, I.H. & Griffiths, R.W. (1990). Implications of mantle plume structure for the evolution of flood basalts. *Earth and Planetary Science Letters* **99**, 79–93.
- Cande, S.C., Searle, R.C. & Hill, I. (1985). Tectonic fabric of the seafloor near north central Atlantic drill sites. *Initial Reports of the Deep Sea Drilling Program* **82**, 17-33.

- Charlou, J.L., Donval, J.P., Douville, E., Jean-Baptiste, P., Radford-Knoery, J., Fouquet, Y., Dapoigny, A. & Stievenard, M. (2000). Compared geochemical signatures and the evolution of Menez Gwen (37°50'N) and Lucky Strike (37°17'N) hydrothermal fluids, south of the Azores triple junction on the Mid-Atlantic Ridge. *Chemical Geology* **171**, 49-75.
- Cochran, J.R. & Talwani, M. (1978). Gravity anomalies, regional elevation, and the deep structure of the North Atlantic. *Journal of Geophysical Research* **83**, 4907-4924.
- Davies G.F. (1999). *Dynamic Earth: Plates, Plumes and Mantle Convection*. Cambridge Univ. Press, Oxford, 458 pp.
- DeMets, C.R., Gordon, R.G., Argus, D.F. & Stein, S. (1990). Current plate motions. *Geophysical Journal International* **101**, 425-478.
- Detrick, R.S., Needham, H.D. & Renard, V. (1995). Gravity anomalies and crustal thickness variations along the Mid-Atlantic Ridge between 33° and 40°N. *Journal of Geophysical Research* **100**, 3767-3787.
- Donnelly, K.E., Goldstein, S.L., Langmuir, C.H. & Spiegelman, M. (2004). Origin of enriched ocean ridge basalts and implications for mantle dynamics. *Earth and Planetary Science Letters* **226**, 347-366.
- Dosso, L., Bougault, H., Langmuir, C.H., Bollinger, C., Bonnier, O. & Etoubleau, J. (1999). The age and distribution of mantle heterogeneity along the Mid-Atlantic Ridge (31 - 41° N). *Earth and Planetary Science Letters* **170**, 269-286.
- Dupré, B. & Allègre, C.J. (1980). Pb-Sr-Nd isotopic correlation and the chemistry of the North Atlantic mantle. *Nature* **286**, 17-22.
- Dupré, B., Lambret, B. & Allègre, C.J. (1982). Isotopic variations within a single oceanic island: the Terceira case. *Nature* **299**, 620 - 622.
- Fouquet, Y., Charlou, J.-L., Donval, J.-P., Radford-Knoery, J., Costa, I., Lourenço, N. & Tivey, M.K. (1994). A detailed study of the Lucky Strike hydrothermal site and discovery of a new hydrothermal site: Menez-Gwen; preliminary results of the DIVA1 Cruise (5-29 May, 1994). *InterRidge News* **3**, 14-19.
- Fouquet, Y., Ondreas, H., Charlou, J.L., Donval, J.P., Radford-Knoery, J., Costa, I., Lourenco, N. & Tivey, M.K. (1995). Atlantic lava lakes and hot vents. *Nature* **377**, 201.
- Galer, S.J.G. & O'Nions, R.K. (1985). Residence time of thorium, uranium and lead in the mantle with implications for mantle convection. *Nature* **316**, 778-782.
- German, C.R., Parson, L.M. & HEAT Scientific team (1996). Hydrothermal Exploration at the Azores Triple-Junction: tectonic control of venting at slow-spreading ridges? *Earth and Planetary Science Letters* **138**, 93-104.
- Goslin, J., Benoit, M., Blanchard, D., Bohn, M., Dosso, L., Dreher, S., Gente, P., Gloaguen, R., Maia, M., Oldra, J.-P., Ravilly, M. & Thiroit, J.-L. (1999). Extent of Azores plume influence on the Mid-Atlantic Ridge north of the hotspot. *Geology* **27**, 991-994.
- Gracia, E., Charlou, J.-L., Radford-Knoery, J. & Parson, L.M. (2000). Non-transform offsets along the Mid-Atlantic Ridge south of the Azores (38°N - 34°N); ultramafic exposures and hosting of hydrothermal vents. *Earth and Planetary Science Letters* **177**, 89-103.
- Grindlay, N.R., Fox, P.J. & MacDonald, K.C. (1991). Second-order ridge axis discontinuities in the South Atlantic: Morphology, structure, and evolution. *Marine Geophysical Research* **13**, 21-49.
- Hofmann, A.W. (2003). Sampling mantle heterogeneity through oceanic basalts: Isotopes and trace elements. In: Carlson, R.W., Holland, H.D. & Turekian, K.K. (eds) *Treatise on Geochemistry: The Mantle and Core*, pp 61-101, Elsevier, New York.
- Humphris, S.E., Fornari, D.J., Scheirer, D.S., German, C.R. & Parson, L.M. (2002). Geotectonic setting of hydrothermal activity on the summit of Lucky Strike Seamount (37°17'N, Mid-Atlantic Ridge). *Geochemistry, Geophysics, Geosystems* **3**, doi: 10.1029/2001GC000284.
- Ito, G. & Lin, J. (1995). Oceanic spreading center-hotspot inter-actions: constraints from along-isochron bathymetric and gravity anomalies. *Geology* **23**, 657-660.
- Ito, E., White, W.M. & Goepel, C. (1987). The O, Sr, Nd and Pb isotope geochemistry of MORB. *Chemical Geology* **62**, 157-176.
- Krause, D.C. & Watkins, N.D. (1970). North Atlantic crustal genesis in the vicinity of the Azores. *Geophysical Journal of the Royal Astronomical Society* **19**, 261-283.
- Langmuir, C.H., Desonie, D., Reynolds, J., Plank, T., Niu, Y., Bourdon, -L.B., Ferguson, E., Hirose, K., Keller, R., Mandal, G., Monteith, J., Stuart, D. & FAZAR-Team (1993). Intensive rock sampling of 16 ridge segments between 32 and 41°N: preliminary results from shipboard analyses, *Eos* **74** (16) 380.
- Langmuir, C.H., Reynolds, J., Bougault, H., Plank, T., Dosso, L., Desonie, D., Gier, E. & Niu, Y. (1996). A petrological traverse along the Mid-Atlantic Ridge across the Azores hotspot. *Journal Conference Abstracts* **1**, 834-835.

- Langmuir, C.H., Humphries, S., Fornari, D., Van Dover, C., Von Damm, K., Tivey, M.K., Colodner, D., Charlou, J.-L., Desonie, D., Wilson, C., Fouquet, Y., Klinkhammer, G. & Bougault, H. (1997). Hydrothermal vents near a mantle hot spot: the Lucky Strike vent field at 37°N on the Mid-Atlantic Ridge. *Earth and Planetary Science Letters* **148**, 69-91.
- Lin, J., Purdy, G.M., Schouten, H., Sempéré, J.-C. & Zervas, C. (1990). Evidence for focussed magmatic accretion along the Mid-Atlantic Ridge. *Nature* **344**, 627-632.
- Lourenço, N., Miranda, M., Luis, J., Ribeiro, A., Mendes-Victor, L.A., Madeira, J. & Needham, H.D. (1998). Morpho-tectonic analysis of the Azores volcanic plateau from a new bathymetric compilation of the Area. *Marine Geophysical Researches* **20**, 141-156.
- Madeira, J. & Ribeiro, A. (1990). Geodynamic models for the Azores triple junction; a contribution from tectonics. *Tectonophysics* **184**, 405-415.
- Michael, P.J., Forsyth, D.W., Blackman, D.K., Fox, P.J., Hanan, B.B, Harding, A.J, Macdonald, K.C., Neumann, G.A, Orcutt, J.A., Tolstoy, M. & Weiland, C.M. (1994). Mantle control of a dynamically evolving spreading center; Mid-Atlantic Ridge 31-34° S. *Earth and Planetary Science Letters* **121**, 451-468.
- Morgan, W.J. (1971). Convection plumes in the lower mantle. *Nature* **230**, 42-43.
- Nataf, H.-C. (2000) . Seismic imaging of mantle plumes. *Annual Review of Earth and Planetary Sciences* **28**, 391–417.
- Needham, H.D., Voisset, M., Renard, V., Bougault, H., Dauteuil, O., Detrick, R. & Langmuir, C. (1992). Structural and volcanic features of the Mid-Atlantic Rift Zone between 40°N and 33°N. *Eos, Transactions, American Geophysical Union* **73** (43), pp 552.
- Niu, Y., Collerson, K. D., Batiza, R., Wendt, J. I. & Regelous, M. (1999). Origin of enriched-type mid-ocean ridge basalt at ridges far from mantle plumes: the East Pacific Rise at 11°20'N. *Journal of Geophysical Research* **104**, 7067–7087.
- Ondréas, H., Fouquet, Y., Voisset, M. & Radford-Knoery, J. (1997). Detailed study of three contiguous segments of the Mid-Atlantic Ridge, South of the Azores (37°N to 38°30'N), using acoustic imaging coupled with submersible observations. *Marine Geophysical Researches* **19**, 231-255.
- Parson, L., Murton, B.J., Searle, R.C., Booth, D., Evans, J., Field, P., Keeton, J., Laughton, A., McAllister, E., Millard, N., Redbourne, L., Rouse, I., Shor, A., Smith, D., Spencer, S., Summerhayes, C. & Walker, C. (1993). En echelon axial volcanic ridges at the Reykjanes Ridge; a life cycle of volcanism and tectonics. *Earth and Planetary Science Letters* **117**, 73-87.
- Parson, L., Gràcia, E., Coller, D., German, C. & Needham, D. (2000). Second-order segmentation; the relationship between volcanism and tectonism at the MAR, 38°N-35°40'N. *Earth and Planetary Science Letters* **178**, 231-251.
- Ridley, W.I., Watkins, N.D. & MacFarlane, D.J. (1974). *The Ocean basins and margins; Vol. 2, The North Atlantic*. Plenum Press, New York, 483 pp.
- Ritsema, J. & Allen, R.M. (2003). The elusive mantle plume. *Earth and Planetary Science Letters* **207**, 1-12.
- Schilling, J.-G. (1975). Azores mantle blob: rare earth evidence. *Earth and Planetary Science Letters* **25**, 103–115.
- Schilling, J.-G., Zajac, M.R., Evans, Johnston, T., White, W., Devine, J.D. & Kingsley, R.H. (1983). Petrologic and geochemical variations along the Mid-Atlantic Ridge from 29°N to 73°N. *American Journal of Science* **283**, 510–586.
- Schilling, J.-G. (1985). Upper mantle heterogeneities and dynamics. *Nature* **314**, 62–67.
- Searle, R. (1980). Tectonic pattern of the Azores spreading centre and triple junction, *Earth and Planetary Science Letters* **51**, 415-434.
- Sempéré, J.C., Brown, H.S., Lin, J., Schouten, H. & Purdy, G.M. (1993). Segmentation and morphotectonic variations along a slow-spreading center: The Mid-Atlantic Ridge (24°N and 30°4N). *Marine Geophysical Research* **15**, 153–200.
- Sinha, M.C. & Loudon, K.E. (1983). The Oceanographer fracture zone: I. Crustal structure from seismic refraction studies. *Geophysical Journal of the Royal Astronomical Society* **75**, 713-736.
- Sleep, N.H. (1990). Hotspots and mantle plumes; some phenomenology. *Journal of Geophysical Research* **95**, 6715-6736.
- Smith, W.H.F. & Sandwell, D.T. (1997). Global sea floor topography from satellite altimetry and ship depth soundings. *Science* **277**, 1956-1962.
- Sun, S.-S. & McDonough, W.F. (1989). Chemical and isotopic systematics of oceanic basalts: implications for mantle composition and processes. In: Saunders, A.D. & Norry, M.J. (eds) *Magmatism in the Ocean Basins*. *Geological Society of London Special Publication* **42**, 313–345.
- Turner, S., Hawkesworth, C., Rogers, N. & King, P. (1997). U–Th isotope disequilibria and ocean island basalt generation in the Azores. *Chemical Geology* **139**, 145 - 164.

- White, W.M. & Schilling, J.-G. (1978). The nature and origin of geochemical variation in Mid-Atlantic Ridge basalts from the Central North Atlantic. *Geochimica et Cosmochimica Acta* **42**, 1501–1516.
- White, W.M., Schilling, J.-G. & Hart, S.R. (1976). Evidence for the mantle plume from Sr isotope geochemistry of the central North Atlantic. *Nature* **263**, 659-662.
- White R.S & McKenzie D. (1989). Magmatism at rift zones: the generation of volcanic continental margins and flood basalts. *Journal of Geophysical Research* **94**, 7685–7729.
- Yu, D., Fontignie, D. & Schilling, J.-G. (1997). Mantle plume-ridge interactions in the central North Atlantic; a Nd isotope study of Mid-Atlantic Ridge basalts from 30°N to 50°N. *Earth and Planetary Science Letters* **146**, 259-272.
- Zhang, Y.-S. & Tanimoto, T. (1992). Ridges, hotspots and their inter-action as observed in seismic velocity maps. *Nature* **355**, 45–49.
- Zhao, D. (2001). Seismic structure and origin of hotspots and mantle plumes. *Earth and Planetary Science Letters* **192**, 251–265.

MERGULHO L12D10

L12D10 Terceira

	LAT	LON	Depth	Date/Hour
Start	38° 38.7190 N	27° 15.0433 W	1906	05.09.12 / 18:31
Finish	38° 52.2104 N	27° 34.0322 W	1918	05.09.12 / 22:50

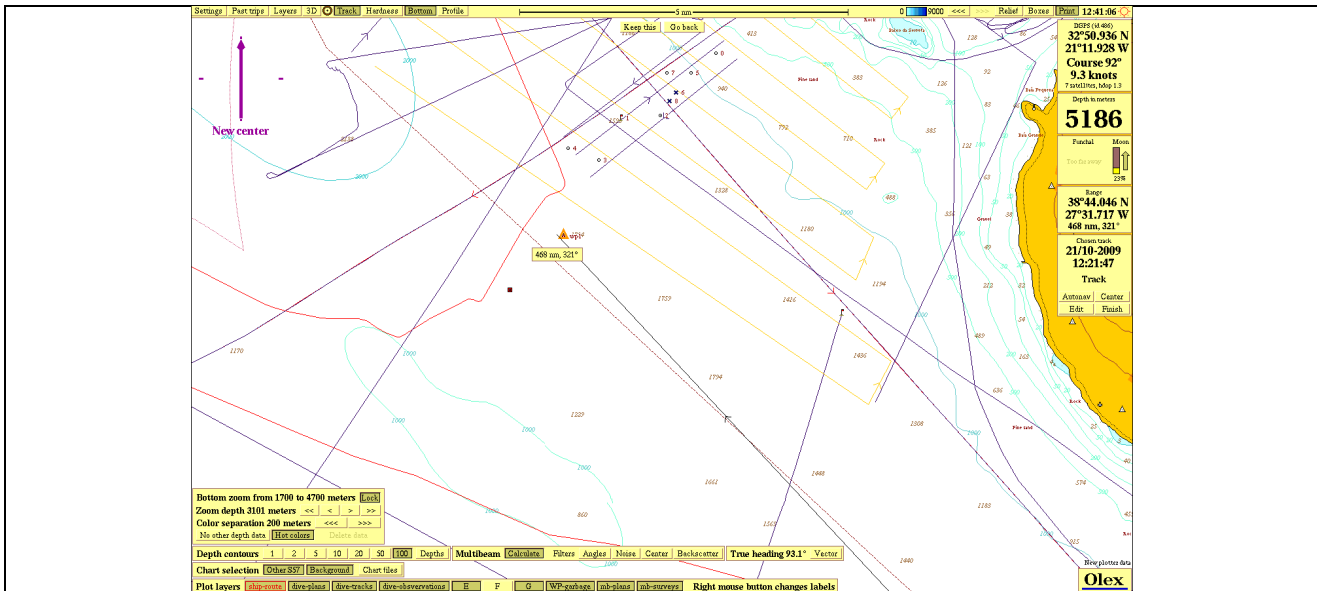


Figure 1. OLEX map depicting wp1 (waypoint 1) position during the dive

Summary

The ROV landed at 20:11 on the seafloor composed of pillow lavas partially covered with sediment. This sediment is whitish, pelagic. Pillow lavas seem fresh and depict striation marks on their glassy rims.

The HD camera had several problems that resulted in several periods with no image capture precluding further scientific observations. The fact that this was merely a test dive also limited the extent of survey in the area; the ROV remained in the same area.

It was still possible to sample two rock samples from adjacent, fresh, glass-covered pillow lavas and sample seawater during the ROV recovery.

ROV Operations

SAMPLING					DATA COLLECTION	
Rock	Sediment Corer	Suction Sampling	Biological	Fluid	Files	Y/N
L12D10R01				L12D10N01	CTD	
L12D10R02				L12D10N02	CH ₄	
				L12D10N03	CO ₂	
				L12D10N04	Olex Img	
					Tracklink	
					Log Pilot	
					Log Tech	
					Sonar	



	LAT	LON	Depth	TIME (GPS)	DATE	# SAMPLES	R	C	S	N	B	b
Start	38°38.7190 N	27°15.0433 W	1906	18:31	5.09.12	6	2				4	
Finish	38°51.0724 N	27°34.0322W	1918	22:50								

TIME (GPS)	LAT	LON	DEPTH (m)	HEADING	OBS.	Sampling
18:31:57	38° 38.7190 N	27° 15.0433 W			ROV in the Water - Start of test dive D10	
					Rocky surface with thin pelagic sediment cover: pillow lavas on a slope	
18:33:00	38° 51.0534 N	27° 33.0992 W	25	255	jellyfish (cnidaria)	
18:34:00	38° 51.0534 N	27° 33.0992 W	57	255	jellyfish (cnidaria)	
18:46:00	38° 51.0382 N	27° 34.0131 W	152	237	zooplankton	
19:17:00	38° 51.0548 N	27° 34.0156 W	641	257	worm (polychaeta)	
19:43:09	38° 51.0762 N	27° 34.0006 W	1244	252	water column	
20:11:00	38° 51.0612 N	27° 33.9966 W	1906	251	ROV on the seabottom: porifera, crustacea	
20:17:00	38° 51.0748 N	27° 33.9964 W	1909	250	mictofideo, rocks with sponges (hexactinellida) and other sponges and several coral	
20:17:21	38° 51.0729 N	27°33.9890 W	1909	253	Fresh pillow lavas with thin pelagic sediment cover	
20:21:00	38° 51.0742 N	27° 33.9974 W	1911	257	Anguiliformes	
20:24:00	38° 51.0838 N	27° 34.0041 W	1915	258	mictofideo, porifera, coral, tube worm, shrimp (crustacea)	
20:33:00	38° 51.0825 N	27° 33.9977 W	1917	285	Several rocks with porifera and coral, sticophate, and some red shrimp (crustacea).	
20:45:00	38° 51.0888 N	27° 34.0032 W	1917	262	rocks with coral	
20:49:00	38° 51.0797 N	27° 34.0032 W	1914	261	red shrimp	
20:53:00	38° 51.0835 N	27° 33.9935 W	1917	254	rocks with coral and sponges	
20:54:00	38° 51.0835 N	27° 33.9935 W	1918	254	Rock with coral. Sponges on the rocks, hexactinellida.	
20:56:38	38° 51.0859 N	27° 33.992 W	1918	251	Tip of a pillow basalt	L12D10R1

TIME (GPS)	LAT	LON	DEPTH (m)	HEADING	OBS.	Sampling
20:59:00	38° 51.0823 N	27° 33.994 W	1918	253	Tip of pillow basalt, next to the one before	L12D10R2
21:08:14	38° 51.0843 N	27° 33.997 W	1918	253	Niskin bottle 1	L12D10N1
22:15:00	38° 51.06 N	27° 34.01 W	600		Niskin 2 - failed	L12D10N2
22:30:00	38° 51.0557 N	27° 34.0365 W	200		Niskin 3	L12D10N3
22:35:00	38° 51.0724 N	27° 34.0322W	100		Niskin 4	L12D10N4
22:36:00					No video display for most of the dive. Hardly any info to do a more complete report.	
22:46:00					end of dive	
22:50:00					ROV on deck	

a



b



c



d



e



f



Basalt L12D10R01

LAT	LON	Depth	Date
38°51.0859 N	27°33.992 W	1918 m	05.09.2012



Morphology	Tip of Pillow Lava	Mass	Aprox. 1 Kg (2 frag.)
Age (0-4)	1	Size	11x9x6 / 5x5x3 cm

External Surface

Glass	Fe-OH	Mn-OH	Palagonite
2/3	Concentric layers		1/3

Phenocrysts

Oxide		Olivine	Plag	Cpx
Y/N	N	Y	Y	?
%		<1%	< 3%	
Size		2 mm	0.1 – 5 mm	
Shape		euhedral	Sub to euhedral	

Matrix

Glassy	Cryptoxl	Massive	% area
Y (vesicles)	Y	N	10/ 90/ 0 %

Vesicles

%	Size	Shape	Distribution
< 3%	Up to 3 mm	coalesced	Concentric.

Fractures

Y/N	%	Precipitates
N		

Remarks/Alteration

Precipitates in vesicle walls (rare), likely zeolites.
 Relatively fresh basalt sample (glassy surface) with partial palagonitization on the glass surface and layered concentric oxidation patterns indicative of subtle alteration. Vesicles are preferentially concentrated on the core of the pillow lava tip.

Basalt L12D10R02

LAT	LON	Depth	Date
38°51.0823 N	27°33.994	1918 m	05.09.2012



Morphology	Pillow Basalt	Mass	Aprox. 2 Kg
Age (0-4)	1	Size	12x12x12 cm

External Surface

Glass	Fe-OH	Mn-OH	Palagonite
	50%		

Phenocrysts

	Oxide	Olivine	Plag	Cpx
Y/N	N	Y	Y	N
%		3%	2%	
Size		1 to 4 mm	1 to 4 mm	
Shape		Sub to euhedral	Sub to euhedral	

Matrix

Glassy	Cryptoxtl	Massive	% area
		Y	

Vesicles

%	Size	Shape	Distribution
20%	I (up to 1 cm); II (less than 1 mm diam)	I (coalesced); II spherical	I (heterogeneous); II (homogeneous)

Fractures

Y/N	%	Precipitates
Y	1-2%	No filling

Remarks/Alteration

Fresh pillow lava sampled from a large size outcrop of pillow blocks with glassy surfaces. Sample R1 belongs to the same outcrop. Visible plagioclase and olivine intergrowths of plagioclase. Two vesicle generations: (I) forming large heterogeneous coalesced groups with glassy walls; (II) a second generation of vesicles (small, only visible with higher magnification) homogeneously distributed in the sample. Fresh sample; good for chemical analysis.

MERGULHO L12D11

L12D11 East of OH3 segment

	LAT	LON	Depth	Date/Hour
Start	33°52.2538 N	36°51.5716 W	1470	10.09.12 / 9:42
Finish	33°52.2104 N	36°51.5880 W	1474	10.09.12 / 14:25

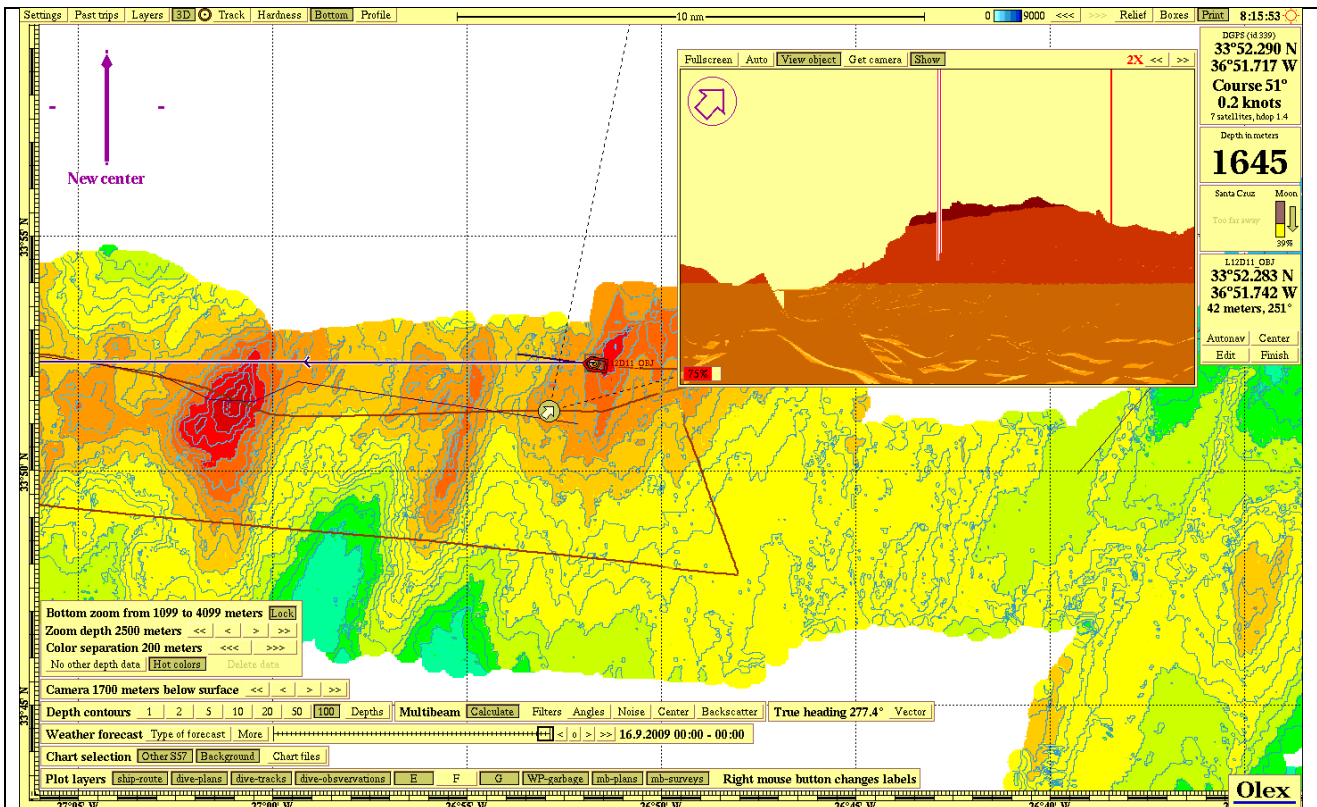


Figure 1. OLEX map with ship's position at starting point

Summary

The ROV landed at 12:00 on top of a rocky surface with approximately 80% rock and 20% sediment. The sediment is whitish/pale yellow.

It was extremely difficult to find a suitable rock fragment to sample. Many, if not all, were strongly attached to the substrate. One rock sample (L12D11R01) was recovered however, technical problems with the ROV's sample box (that has fallen) resulted in losing the sample. Several other attempts to sample rocks failed due to the extremely hard/massive nature of the outcrops. Lineaments (marked as polished surfaces) on the rock surfaces (Photo P), visible vein-like textures (Photos D, I) and overall looks of the massive looking outcrops (Photo S) may be indicators of this being a core complex (???) with mafic and/or ultramafic rocks (??).

In this area volcanic rocks are dominant relatively to sediments, although some zones may show more than 60% sediment, preferentially in areas where the slope is less accentuate. This sediment is white to pale yellow in color. Two different type of volcanic facies are identified:



(1) volcanic rocks forming more massive and planar shapes that could correspond to lobate type flows, indicative of a more lava production. This type of lavas seems to be relatively old (no glass on the surface and showing some external alteration visible by the existence of brownish – reddish alteration materials on some of the external layer). In some areas, where they form true planar outcrops (partially covered by the with-light yellowish sediment) they show a foliation on the surface. The attempts to collect a second volcanic sample didn't have any success because even the edge of the outcrops were impossible to break, meaning, probably, that they were very cohesive. In some images, it seems that some of these lavas are fractured (irregularly in shape) and filled by sediment.

(2) The second volcanic type identified are the pillow lavas that outcrop either as dispersed rounded fragments or as accumulation of them. They are also very massive pillows, and relatively old too (as the lobates). Heterogeneously dispersed. Cross-section of broken rounded fragments show a radial internal structure.

The area explored in this dive, morphologically is part of a slope (some images (~13.09 gps time; allows to see the orientation for it of 022° azimuth) that show zones of variable slope: the volcanic outcrops clearly dominate in the more steep slopes, whereas the sediment is more frequent (up to more than 60% in area) in the lower slopes. Given the huge amount of volcanic it seems that this is a constructional slope, made preferentially by lobate type of flows, although the existence of dispersed (some times more frequent) pillow lavas. We could imagine a higher lava production (lobate flows) that ends with the pillow lavas (lower lava production rate).

ROV Operations

SAMPLING					DATA COLLECTION	
Rock	Sediment Corer	Suction Sampling	Biological	Fluid	Files	Y/N
L12D11R1 (lost)				L12D11N01 L12D11N02	CTD CH ₄ CO ₂ Olex Img Tracklink Log Pilot Log Tech Sonar	

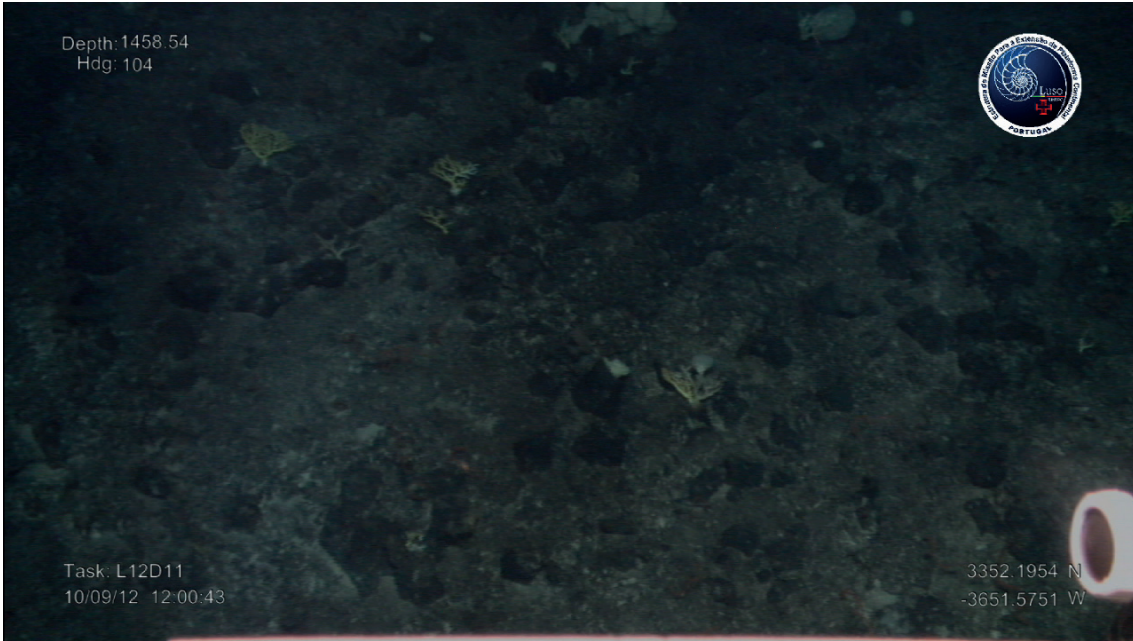


	LAT	LON	Depth	TIME (GPS)	DATE	# SAMPLES	R	C	S	N	B	b
Start	N 33° 52.2006	W 36° 51.5709	1459.54 m	12:02:00	10.09.12	2				2		
Finish	N 33° 52.2109	W 36° 51.5864	1468 m	13:18:00	10.09.12							

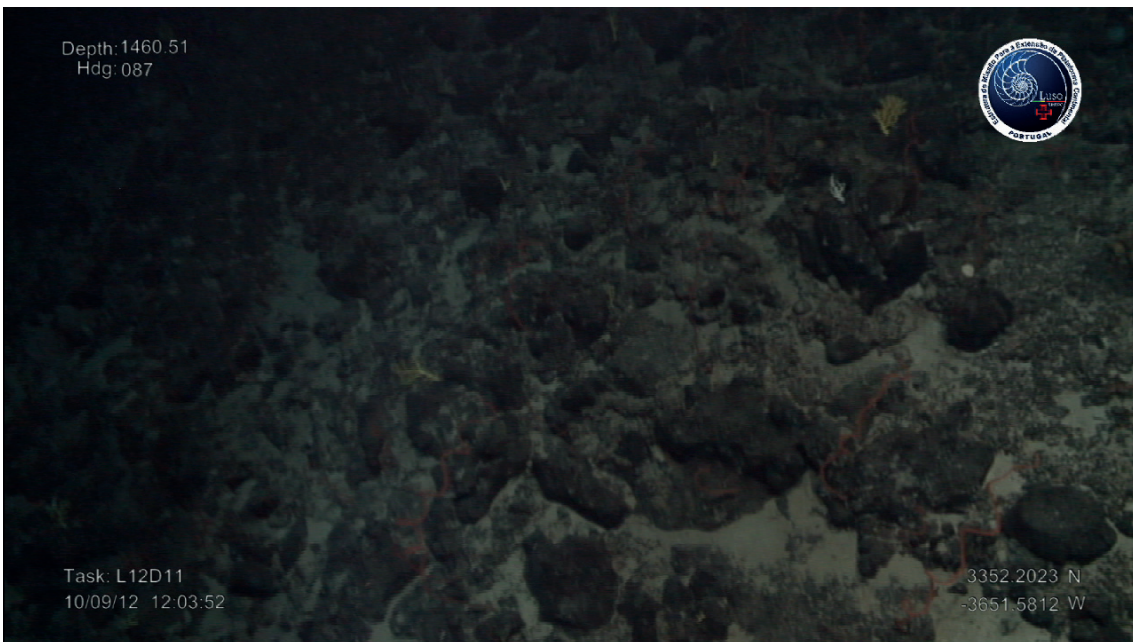
TIME (GPS)	LAT	LON	DEPTH	HEADING	OBS.	Sampling
9:42:07	3352.2337 N	36°51.5590 W	0	65	Start D11	
9:42:24	3352.2337 N	36°51.5590 W	0	65	ROV on the water	
9:52:17	3352.2448 N	36°51.5561 W	100	69	Zooplankton	
10:01:00	33°52.2416 N	36°51.5550 W	186,46	42	Going down	
10:22:00	3352.2282 N	36°51.5091 W	367	85	Worm	
10:57:00	3352.2514 N	36°51.5982	644	65	Cnidaria (jellyfish)	
12:02:00	3352.2006 N	36°51.5709	1459,54	85	ROV on the ground. Several Coral (FIG_12a), several porifera(FIG_11b), several sticopathes(red and white)(FIG_13), several gorgonia (FIG_12), sea urchin (equinodermata) (FIG_11b), tunicata, crustacea (red shrimp)(FIG_15), pink coral(FIG_16), equinodermata(sea star)(Fig_18), huge white porifera(FIG_17), polichaeta (tube worms)(FIG_11b), gastropoda(FIG_13).	PN1
12:00:00	33°52.2011 N	36°51.5779 W	1457	96	Pillow Outcrop partially covered by sediment. Gently slope.	
12:03:00			1460	86	80% pillow outcrop, the rest is sediment. Gentle slope oriented 100°.	
12:05:00			1462	84	The shape of the pillows sometimes are not so clear! Slope more horizontal. Rov on the bottom to sample. Partially covered by sediment (10-20%). Cross section of the rounded fragments show a radial internal structure.	
12:06:00	33°52.1922 N	36°51.5793 W	1462		Detail of rock outcrop where veins are visible at the rock surface as positive reliefs.	
12:13:00	33°52.193 N	36°51.5784 W	1467	66	Still in the same area. More massive volcanic blocks of irregular shape. The lavas seems old and fragmented. 10% sediment.	
12:17:00			1468	62	Rov arm in action for sampling. Some of the fragments show a brownish/redish coloration on the surface - alteration. The majority of the fragments rounded. In some of them, trasversal cuts shown radial structure.	
12:19:45	3352.1959 N	36°51.58.23	1468	70	sample of rock(FIG_22), brittle star(FIG_29) , tube worm(FIG_31), crustacea(FIG_29) , sea urchin (FIG_30)	L12D11R1(lost)
12:25:00			1471	64	small rounded sample collected.	
12:30:00					Sample box fell off ROV	
12:33:00	33°52.1551 N	36°51.6843 W	1470		80% rock, 20% soft white/yellowish sediment; outcrops of massive melanocratic blocks that seem loose but aren't.	L12D11R1 (lost)
13:04:00			1468	12	Trying to collect another sample. Massive rounded fragments that passes to a more massive sheet flow? Outcrop.	
13:05:00	3352.2137 N	36°51.5648 W	1467	20	sponges (hexactinellidae)(FIG_32), coral(FIG_32)	
13:07:00			1470	3	Again a zone with more rounded, pillow lavas, covered partially by sediment. The same old and massive aspect.	

TIME (GPS)	LAT	LON	DEPTH	HEADING	OBS.	Sampling
13:09:00			1475	47	Sleep slope. It seems that we are in the base of this slope with a orientation of 022° azimuth. Sediment more frequent (up to more than 60%) in some areas.	
13:09:00	3352.2228 N	36°51.5805 W	1475	26	crustaca, sea urchin(FIG_33), gorgonia(FIG_33), sticopathes(FIG_28), sea anemone (cnidaria)(FIG_28)	
13:12:00	33°52..2279	36°51.5886 W	1474	29	Where the lava outcrops are more frequent these are massive, sometimes having dispersed some rounded and small (< m) blocks. In general it seems that we are in a constructional ridge. The more massive flows show a foliation.	
13:13:00	33°52.2279N	36°51.5886 W	1474		Sample box has fallen. Lost the sample. One tried to sample once again but all the "loose" blocks are in fact part of the outcrop. There are visible lineaments as polished surfaces in some of the rock surfaces. Veinlike textures on the rock surfaces. A large outcrop with a face NNW-SSE shows one large horizontal layer/fracture. This might be a core complex and rocks might not be basalts.	
13:18:00	3352.2109 N	36°51.5864 W	1468	92	Branched coral white and brown(FIG_27), several huge sponges (Hexactinellidae)(FIG_17)	
13:20:00			1468	48	Continuing to try to sample a second volcanic. Some of the more flattened outcrops seems to be very hard to break.	
13:21:00	33°52.2104 N	36°51.5880 W			Going up	
13:31:30	3352.1848 N	36°51.5838 W	1321	53	Niskin 1	L12D11N1
13:45:00	3352.2258 N	36°51.5744 W	920	26	brown fish	
13:59:35	3352.2243 N	36°51.5434 W	583	21	Niskin 2	L12D11N2
14:23:00					end of dive	
14:25:00					Rov on deck	

a



b



c



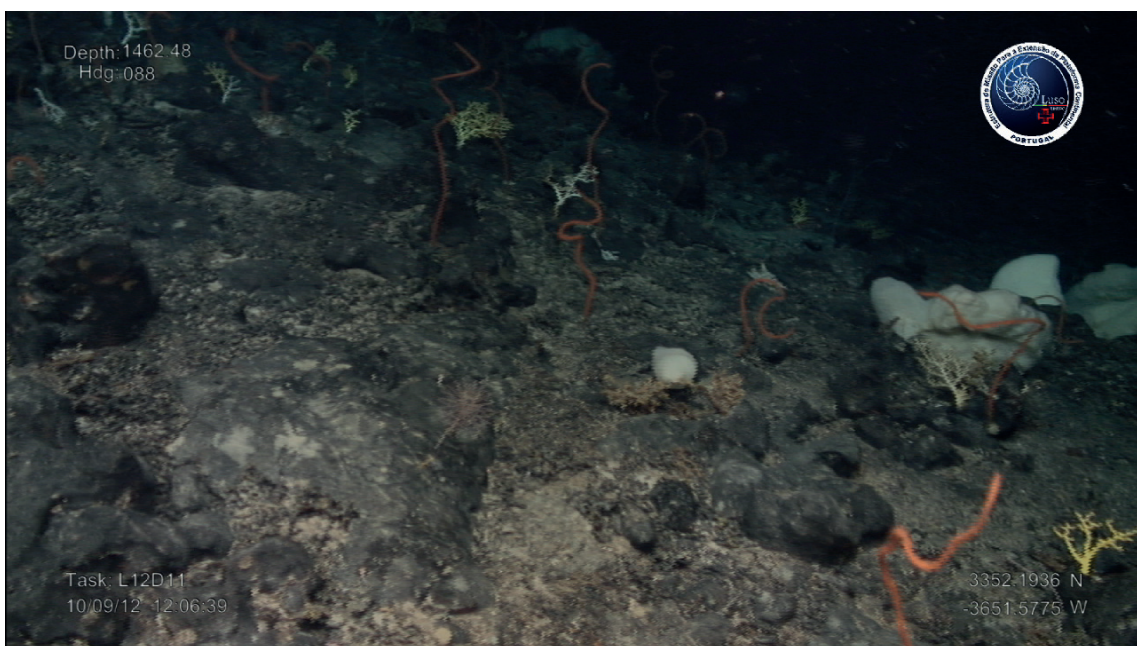
d



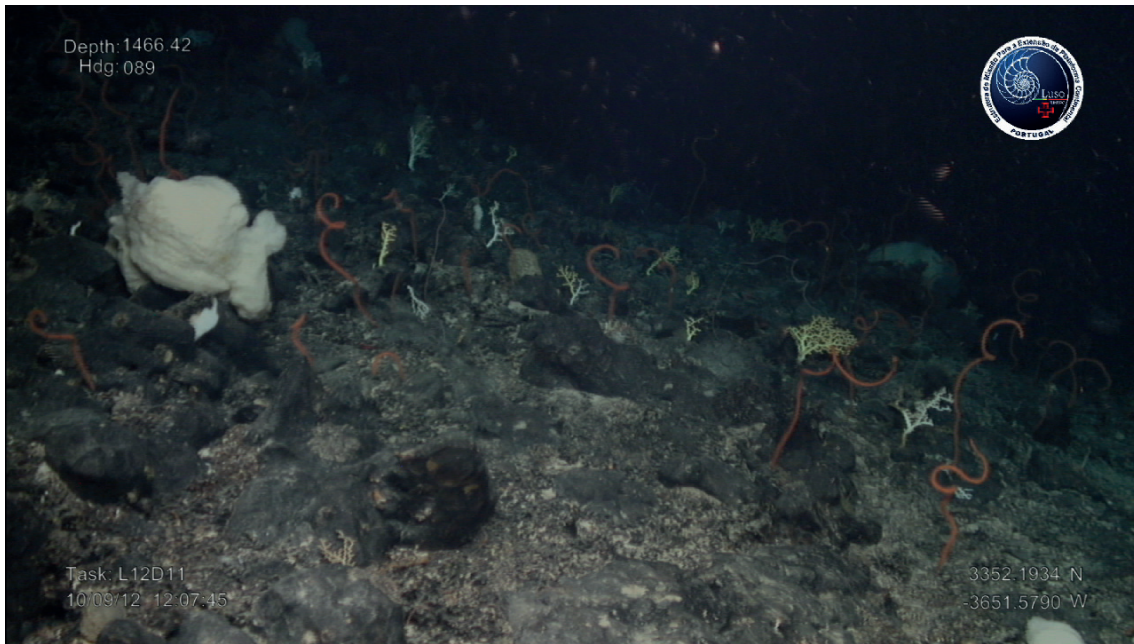
e



f



g



h



i



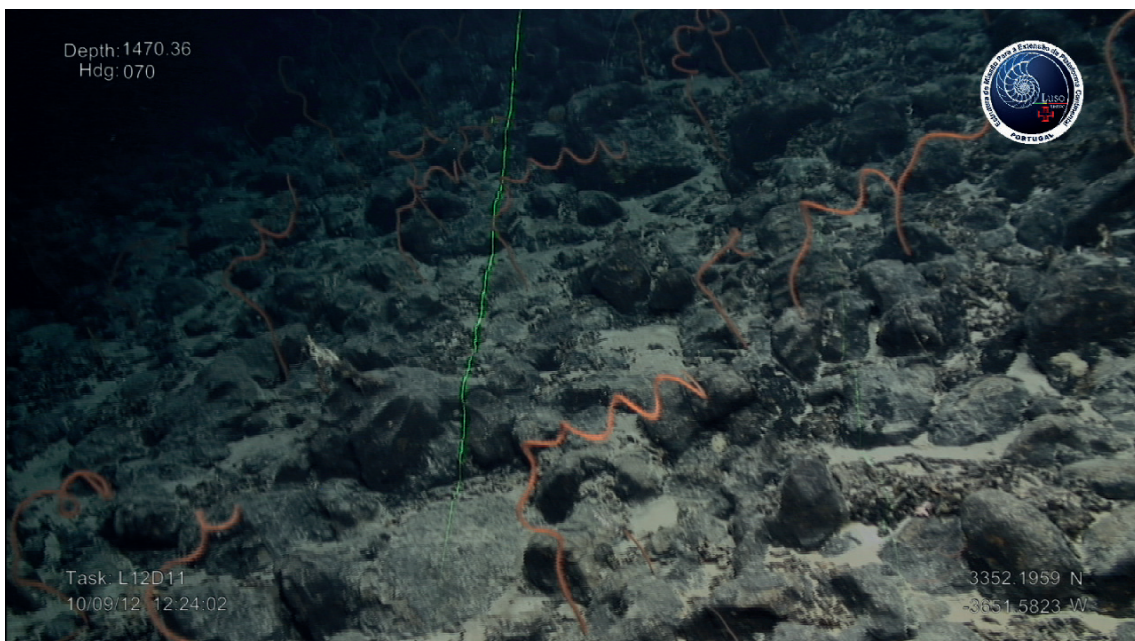
j



k



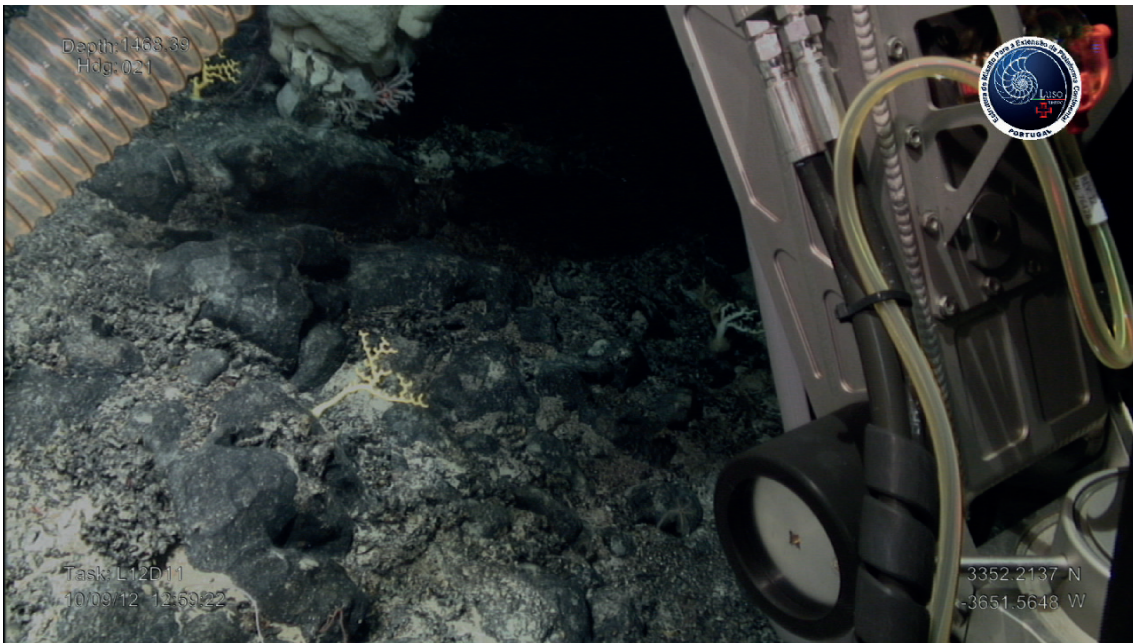
l



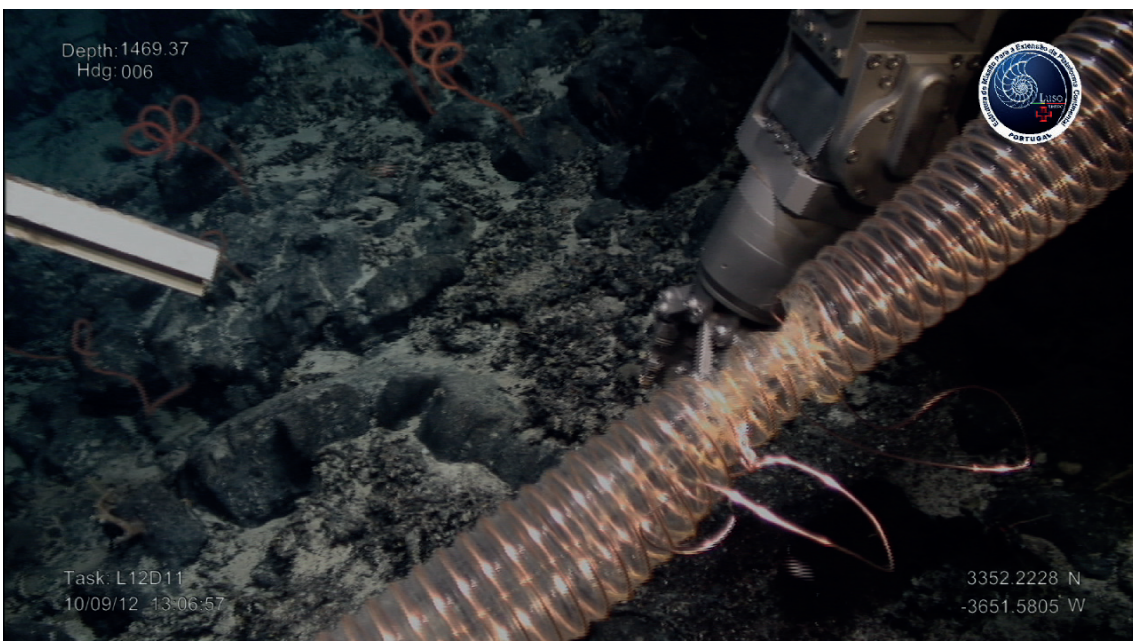
m



n



o



p



q



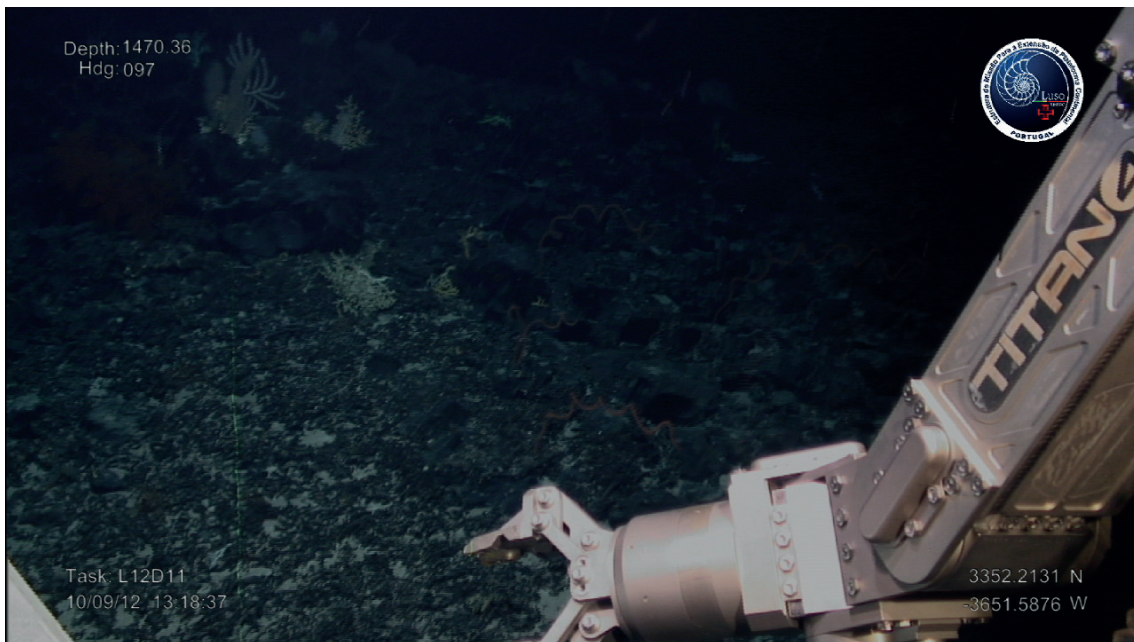
r



s



t



u



MERGULHO L12D12

L12D12 East of OH3 segment

	LAT	LON	Depth	Date/Hour
Start	33°55.0900 N	37°30.3902 W	1143	11.09.12 / 10:11
Finish	33°55.0886 N	37°30.4774 W	1130	11.09.12 / 15:45

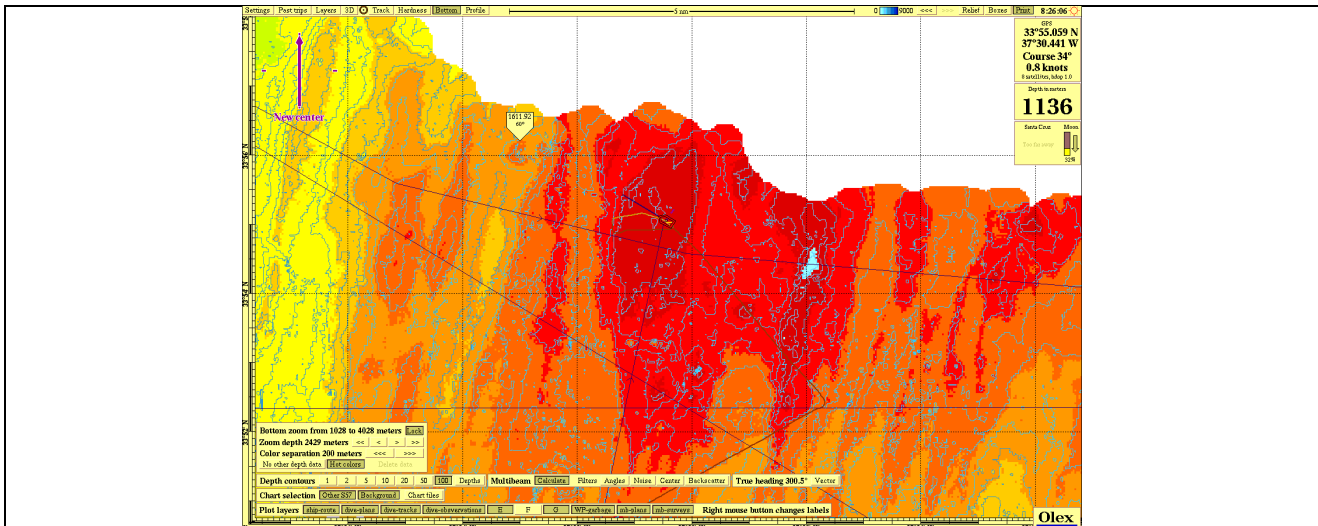


Figure 1. OLEX map with ship's position at starting point

Summary

At approximately 800 m deep the ROV crossed what seemed to be a hydrothermal plume. The CO₂ and turbidity sensors depict a variation in the water column.

The ROV has landed on an altered rocky surface with 60% sediment cover. The area is relatively flat and is covered heterogeneously by white to yellowish sediment with dark particles that may be bioclasts (or siliciclastic material??) (Photo A) interrupted by outcrops of irregular shaped rocks; some having pseudo-planar structures and dark surface. These rocks likely correspond to sediment breccias / sediment crusts (Photo A). Rocks depict a rough surface and fracture pattern with a N50°W trend. Fractured areas on the rock surface show a yellow material whereas their surfaces are reddish to ochre. Most likely these are sedimentary breccias with carbonate fillings that resulted from intense seafloor alteration. One sample was collected; a large block from this sedimentary crust (Photo B; L12D12R01). A tentative suction sampling failed due to rupture of the suction tube broken into three segments (Photo C). However, using the articulated arm we've collected a small volume of this sediment with biological material (Photo D) (L12D12Fundo).

Up the hill large size pillow lavas lay on top of the sedimentary/breccia layers (Fig. E). These pillows are oxidized depicting an ochre color and large fragmentation networks (due to cooling). We left this area and started going up on a gentle slope oriented, approximately NNE-SSW. The domains of sediment + crusts were interrupted by an outcrop of pillow lavas (Photo F). These pillows are rounded (some almost spherical) (Photo G) to elongated (Photo H), outcropping either as isolated pillows (Photo H) or forming small groups (Photo F). Clearly visible the borders of these pillows (Photo I), having brownish colors in the cross sections, but the external surfaces are dark, probably revealing Mn-rich accumulations; or Fe-OH surface alteration (Fig. J) that results in an ochre color on the pillow lava surfaces. Lavas seem to be old in age, and altered. Some pillows have significant dimensions (~1m length); some are fractured, collapsed and others are open



pillows (Photo K). Two volcanic samples were collected 3 meters apart: L12D12R02, the tip of a pillow lava (Photo L, M); L12D12R3, a fragment of a pillow lava rim (Photo N). Continuing going up on the slope, the volcanic outcrops alternate continuously with sedimentary crusts + sediment units. Sometimes the pillow lavas are closely packed (Photo O). However, in some places lava tubes are clearly visible on the sea bottom (Photo P) spatially related with the pillows. This indicates distinct magmatic fluxes occurring in the same area. The dive finished in another pillow lava outcrop, where a fragment was collected (L12D12R4) (Photo Q).

The dive area shows an intercalation of oxidized pillow lavas + lava tubes and sedimentary units the latter with marked fracture networks and layered bands (N50°W; ± 30° SW), other structural features is a marked steep slope on lavas most likely fracture controlled (N20°E; at 13:11) and a crossed pattern of fractures on the sedimentary features (N20°W – N25°E; 13:24). Total time on the bottom: 1 hour and 35 minutes.

ROV Operations

SAMPLING					DATA COLLECTION	
Rock	Sediment Corer	Suction Sampling	Biological	Fluid	Files	Y/N
L12D12R01				L12D12N01	CTD	
L12D12R02				L12D12N02	CH ₄	
L12D12R03				L12D12N03	CO ₂	
L12D12R04				L12D12N04	Olex Img	
					Tracklink	
					Log Pilot	
					Log Tech	
					Sonar	

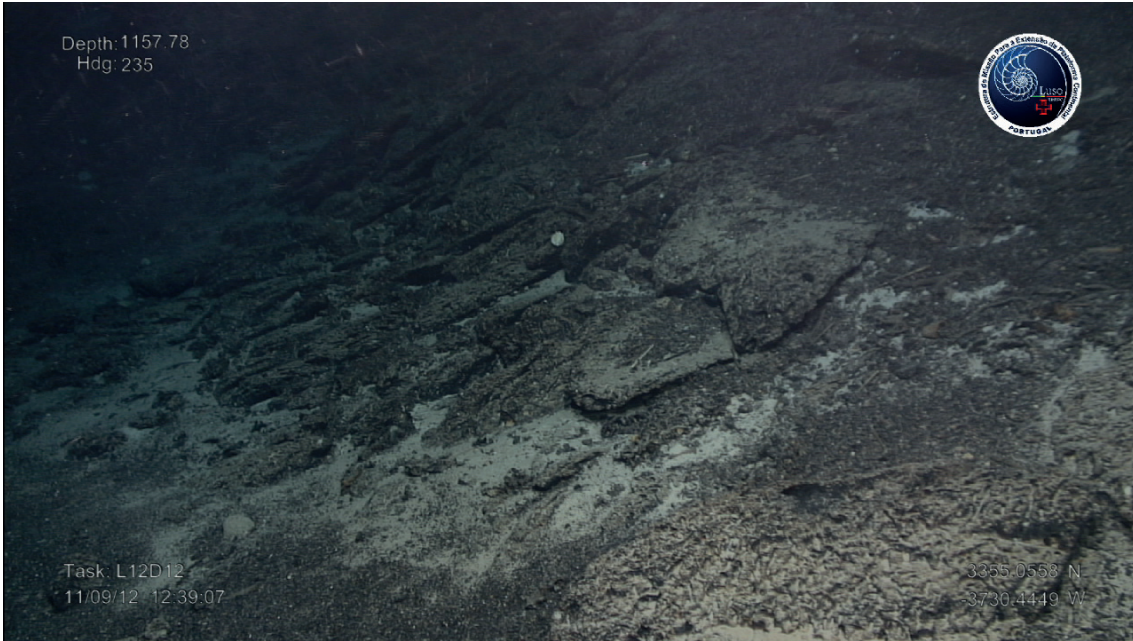


	LAT	LON	Depth	TIME (GPS)	DATE	# SAMPLES	R	C	S	N	B	b
Start	N 33° 52.2006	W 36° 51.5709	1459.54 m	12:02:00	10.09.12	2				2		
Finish	N 33° 52.2109	W 36° 51.5864	1468 m	13:18:00	10.09.12							

TIME (GPS)	LAT	LON	DEPTH	HEADING	OBS.	Sampling
9:42:07	3352.2337 N	36°51.5590 W	0	65	Start D11	
9:42:24	3352.2337 N	36°51.5590 W	0	65	ROV on the water	
9:52:17	3352.2448 N	36°51.5561 W	100	69	Zooplankton	
10:01:00	33°52.2416 N	36°51.5550 W	186,46	42	Going down	
10:22:00	3352.2282 N	36°51.5091 W	367	85	Worm	
10:57:00	3352.2514 N	36°51.5982	644	65	Cnidaria (jellyfish)	
12:02:00	3352.2006 N	36°51.5709	1459,54	85	ROV on the ground. Several Coral (FIG_12a), several porifera(FIG_11b), several sticopathes(red and white)(FIG_13), several gorgonia (FIG_12), sea urchin (equinodermata) (FIG_11b), tunicata, crustacea (red shrimp)(FIG_15), pink coral(FIG_16), equinodermata(sea star)(Fig_18), huge white porifera(FIG_17), polichaeta (tube worms)(FIG_11b), gastropoda(FIG_13).	PN1
12:00:00	33°52.2011 N	36°51.5779 W	1457	96	Pillow Outcrop partially covered by sediment. Gentle slope.	
12:03:00			1460	86	80% pillow outcrop, the rest is sediment. Gentle slope oriented 100°.	
12:05:00			1462	84	The shape of the pillows sometimes are not so clear! Slope more horizontal. Rov on the bottom to sample. Partially covered by sediment (10-20%). Cross section of the rounded fragments show a radial internal structure.	
12:06:00	33°52.1922 N	36°51.5793 W	1462		Detail of rock outcrop where veins are visible at the rock surface as positive reliefs.	
12:13:00	33°52.193 N	36°51.5784 W	1467	66	Still in the same area. More massive volcanic blocks of irregular shape. The lavas seems old and fragmented. 10% sediment.	
12:17:00			1468	62	Rov arm in action for sampling. Some of the fragments show a brownish/redish coloration on the surface - alteration. The majority of the fragments rounded. In some of them, trasversal cuts shown radial structure.	
12:19:45	3352.1959 N	36°51.58.23	1468	70	sample of rock(FIG_22), brittle star(FIG_29) , tube worm(FIG_31), crustacea(FIG_29) , sea urchin (FIG_30)	L12D11R1(lost)
12:25:00			1471	64	small rounded sample collected.	
12:30:00					Sample box fell off ROV	
12:33:00	33°52.1551 N	36°51.6843 W	1470		80% rock, 20% soft white/yellowish sediment; outcrops of massive melanocratic blocks that seem loose but aren't.	L12D11R1 (lost)
13:04:00			1468	12	Trying to collect another sample. Massive rounded fragments that passes to a more massive sheet flow? Outcrop.	
13:05:00	3352.2137 N	36°51.5648 W	1467	20	sponges (hexactinellidae)(FIG_32), coral(FIG_32)	
13:07:00			1470	3	Again a zone with more rounded, pillow lavas, covered partially by sediment. The same old and massive aspect.	

TIME (GPS)	LAT	LON	DEPTH	HEADING	OBS.	Sampling
13:09:00			1475	47	Sleep slope. It seems that we are in the base of this slope with a orientation of 022° azimuth. Sediment more frequent (up to more than 60%) in some areas.	
13:09:00	3352.2228 N	36°51.5805 W	1475	26	crustaca, sea urchin(FIG_33), gorgonia(FIG_33), sticopathes(FIG_28), sea anemone (cnidaria)(FIG_28)	
13:12:00	33°52..2279	36°51.5886 W	1474	29	Where the lava outcrops are more frequent these are massive, sometimes having dispersed some rounded and small (< m) blocks. In general it seems that we are in a constructional ridge. The more massive flows show a foliation.	
13:13:00	33°52.2279N	36°51.5886 W	1474		Sample box has fallen. Lost the sample. One tried to sample once again but all the "loose" blocks are in fact part of the outcrop. There are visible lineaments as polished surfaces in some of the rock surfaces. Veinlike textures on the rock surfaces. A large outcrop with a face NNW-SSE shows one large horizontal layer/fracture. This migh me a core complex and rocks might not be basalts.	
13:18:00	3352.2109 N	36°51.5864 W	1468	92	Branched coral white and brown(FIG_27), several huge sponges (Hexactinellidae)(FIG_17)	
13:20:00			1468	48	Continuing to try to sample a second volcanic. Some of the more flattened outcrops seems to be very hard to break.	
13:21:00	33°52.2104 N	36°51.5880 W			Going up	
13:31:30	3352.1848 N	36°51.5838 W	1321	53	Niskin 1	L12D11N1
13:45:00	3352.2258 N	36°51.5744 W	920	26	brown fish	
13:59:35	3352.2243 N	36°51.5434 W	583	21	Niskin 2	L12D11N2
14:23:00					end of dive	
14:25:00					Rov on deck	

a



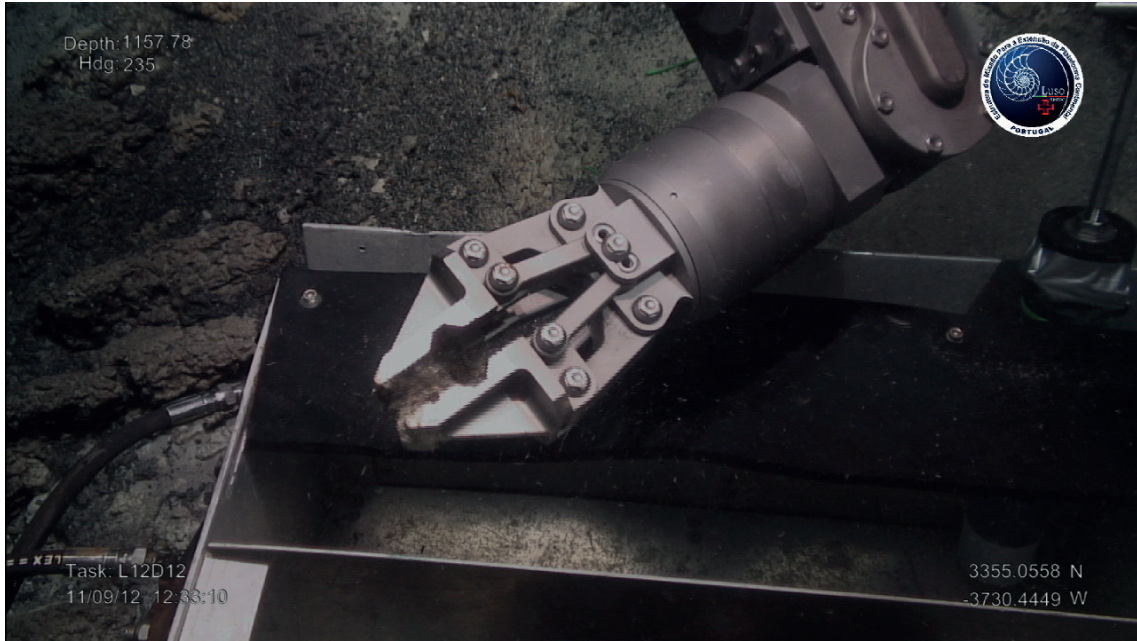
b



c



d



e



f



h



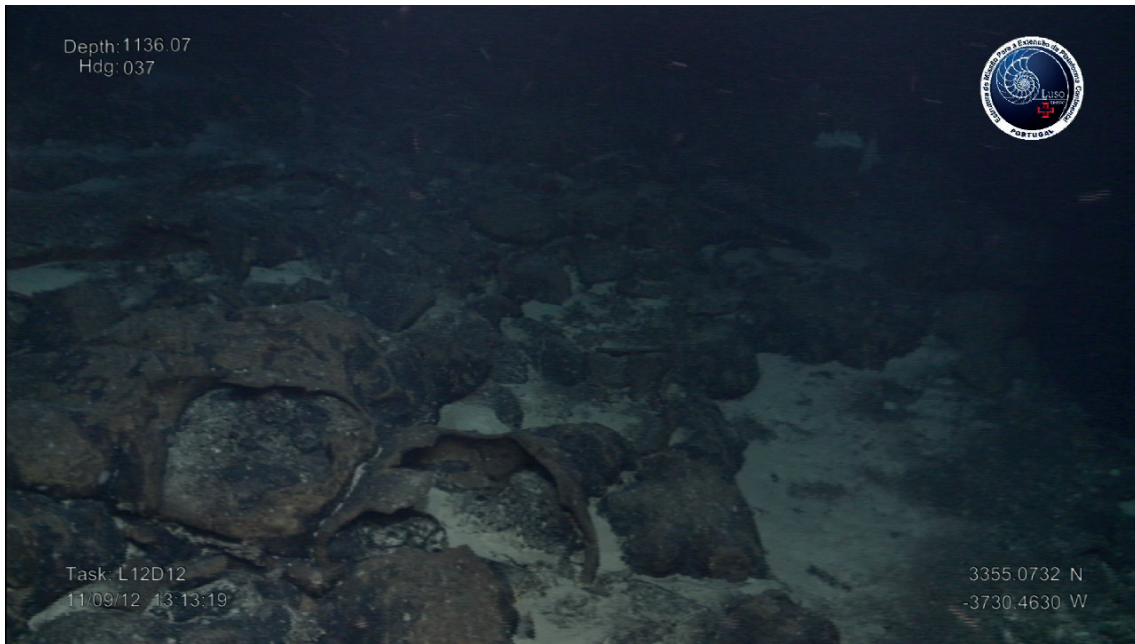
i



j



k



l



m



n



o



p



q



Basalt L12D12R02

LAT	LON	Depth	Date
33°55.0655 N	37°30.4631 W	1144	10.09.12



Morphology	Pillow Lava Bud	Mass	2kg – 3 Kg
Age (0-4)	2	Size	25 x 10 x 10 cm

External Surface

Glass	Fe-OH	Mn-OH	Palagonite
N	80%	20%	

Phenocrysts

	Oxide	Olivine	Plag	Cpx
Y/N	N	Y	Y	N
%		1%	20%	
Size		< 2 mm	1 mm – 1 cm	
Shape			Anhedral to euhedral	

Matrix

Glassy	Cryptoxtl	Massive	% area
	(rare plag laths)	Y	

Vesicles

%	Size	Shape	Distribution
< 2 %	< 1 mm	rounded	homogeneous

Fractures

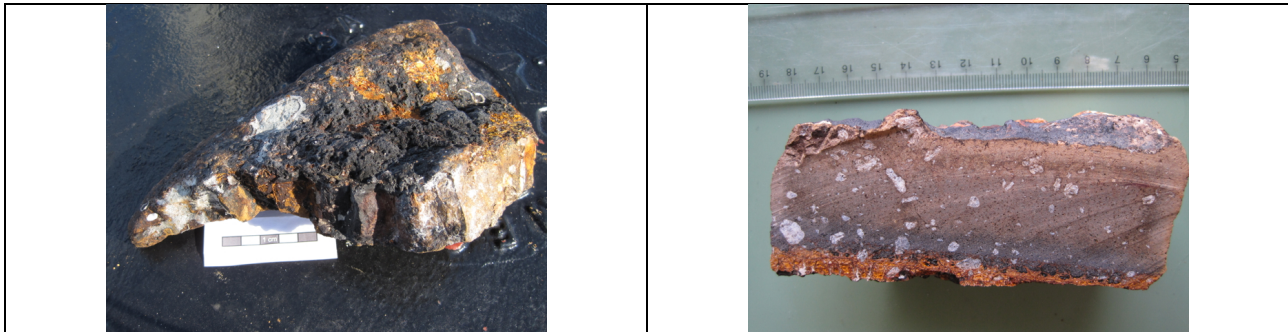
Y/N	%	Precipitates
Y	< 1 %	White material (carb.?)

Remarks/Alteration

Veins filled with white material on the walls and a darker precipitate on the vein core (more recent – open space filling). Olivine is sometimes included on the plagioclase phenocrysts.

Basalt L12D12R03

LAT	LON	Depth	Date
33°55.0655 N	37°30.4631 W	1144	10.09.12



Morphology	Pillow border	Mass	1.5 Kg
Age (0-4)	2	Size	15x12x7 cm

External Surface

Glass	Fe-OH	Mn-OH	Palagonite
<1%	30%	50%	20%

Phenocrysts

	Oxide	Olivine	Plag	Cpx
Y/N		Y	Y	
%		1 %	10%	
Size		< 1 mm	1 mm – 1 cm	
Shape		subhedral	Sub-to euhedral	

Matrix

Glassy	Cryptoxl	Massive	% area
		Y	

Vesicles

%	Size	Shape	Distribution
<3%	<1 mm	circular	homogeneous

Fractures

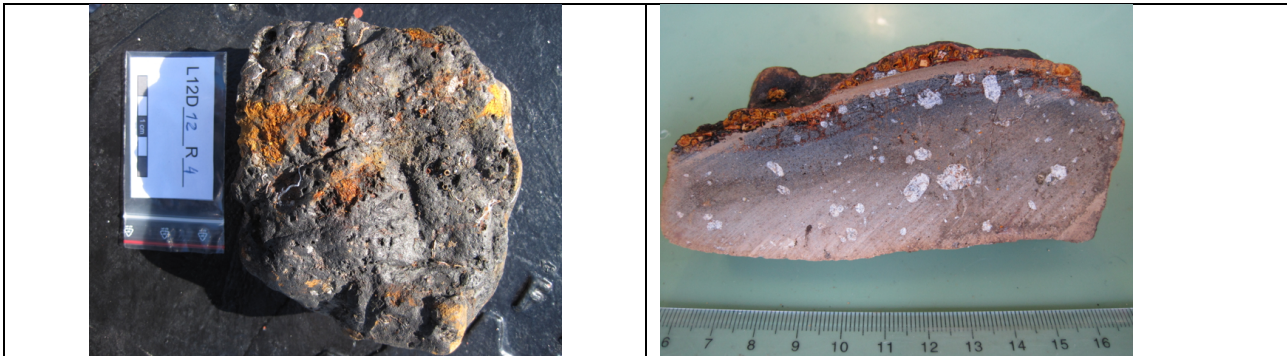
Y/N	%	Precipitates
Y		Y dark vitreous material

Remarks/Alteration

The external surface is essentially made by Mn-OH deposits but also containing Fe-OH material (brownish colored). However, a cross cut of the fragment reveals an external border of alteration having about 5 mm thick (ochre-brownish colored) whereas small individual pieces of unaltered glass (up to 4 mm in length) are still found. Part of the ochre colored mass is Palagonite and the more massive material is Fe-OH deposit.

Basalt L12D12R04

LAT	LON	Depth	Date
33°55.0886 N	37°30.4774 W	1130	10.09.12



Morphology	Rim of pillow	Mass	1 Kg
Age (0-4)	2	Size	10 x 12 x 5 cm

External Surface

Glass	Fe-OH	Mn-OH	Palagonite
Y 5 %		70 %	25%

Phenocrysts

Oxide	Olivine	Plag	Cpx
Y/N	Y	Y	
%	< 1 %	15 %	
Size	< 1 mm	1 mm – 7 mm	
Shape	subhedral	Anhedral to subhedral	

Matrix

Glassy	Cryptoxl	Massive	% area
		Y	

Vesicles

%	Size	Shape	Distribution
< 2 %	1 mm	rounded	homogeneous

Fractures

Y/N	%	Precipitates
Y		Filled with white material (carb?) and dark vitreous material

Remarks/Alteration

Similar to L12D12R03 but it has more glass on the alteration rim and external surface almost completely covered by Mn-oxide material. Some vesicles show precipitates on the walls. Olivine included in plagioclase phenocrysts.

MERGULHO L12D13

L12D13

S of Hayes, E of MAR

	LAT	LON	Depth	Date/Hour
Start	33° 27.2253 N	38° 57.2752 W	1546	13.09.12 / 10:57
Finish	33° 27.1748 N	38° 57.3165 W	1488	13.09.12 / 16:36

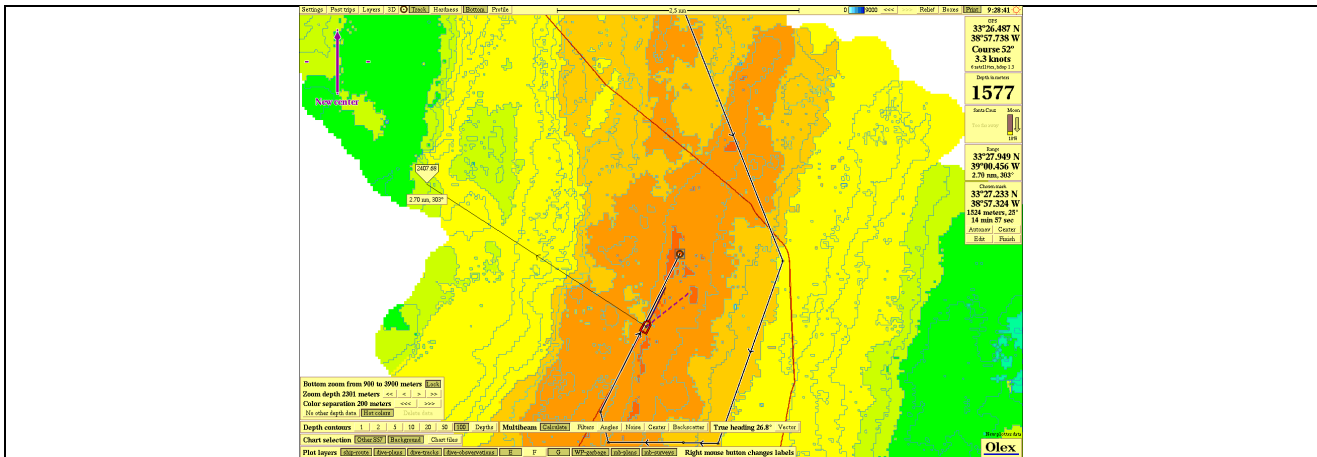


Figure 1. OLEX map with ship's position and starting point

Summary

The ROV landed at the sea bottom at 12:24. The seafloor surface is relatively flat and completely covered by sediment (whitish – pale yellowish colored) (Photo A). Limestone aggregates rocks are heterogeneously dispersed in the sediment (Photo B); these rocks depict a dark brown to black alteration cap with a breccia-like surface and lay on the surface producing a small relief relatively to the sediment (Photo C). At 12:48 the roV headed 280-290° towards the top of the slope where is visible an outcrop of isolated pillow lavas and some lava tubes (Photo D). Both types of volcanic have very irregular shapes, and the rims of the lavas often show buds or protrusions (Photo E). The lavas are isolated in the sediment or, more frequent, constitute agglomerates of individual pillows or lava tubes (Photo F). The sediment is almost all time present (<20% to 50% area). Areas with less sediment cover, and with large pillow outcrops have steeper slopes, probably corresponding to minor haystacks (small mounds) (in the vicinity of these constructional structures there is a general increase in the lava tubes morphology) (Photo G). The majority of pillow lavas may be in reality, tips of lava tubes (Photo H) that are partially covered by sediment. Morphologically, these lava tubes are very irregular in shape and in dimensions (< than 50 cm to more than 2-3 m long, with proportional increase in the corresponded diameter) (Photos I and J). They constitute massive lavas, very hard to sample (many attempts were made to sample but with small success). The samples collected were either rims (sample L12D13R3) (Photo K) of the lavas or the most prominent protrusions - samples L12D13R1, L12D13R2 (Photo M and N), L12D13R4 (Photo O) and L12D13R5 (Photo P). Outcrops of volcanics, irregularly covered by variable sediment proportions, intercalated with areas of more sediment having, or not, the sedimentary crusts. The final stage of the dive is impressive, reaching the summit of the haystack (Photo Q, R) – what appears to be the main volcanic vent, a well-developed, constructional front. In this summit, small tabular sheet flows are also outcropping, together with the well-developed lava tubes (Photo S).

ROV Operations

SAMPLING					DATA COLLECTION	
Rock	Sediment Corer	Suction Sampling	Biological	Fluid	Files	Y/N
L12D13R01	L12D13C01			L12D13N01	CTD	
L12D13R02				L12D13N02	CH ₄	
L12D13R03				L12D13N03	CO ₂	
L12D13R04					Olex Img	
L12D13R05					Tracklink	
					Log Pilot	
					Log Tech	
					Sonar	



	LAT	LON	Depth	TIME (GPS)	DATE	# SAMPLES	R	N	C	S	B	b
Start	33° 27.2253 N	38° 57.2752 W	1546 m	12:28	13.09.12	10	5	3	1			
Finish	33° 27.1748 N	38° 57.3165 W	1488 m	15:58	13.09.12							

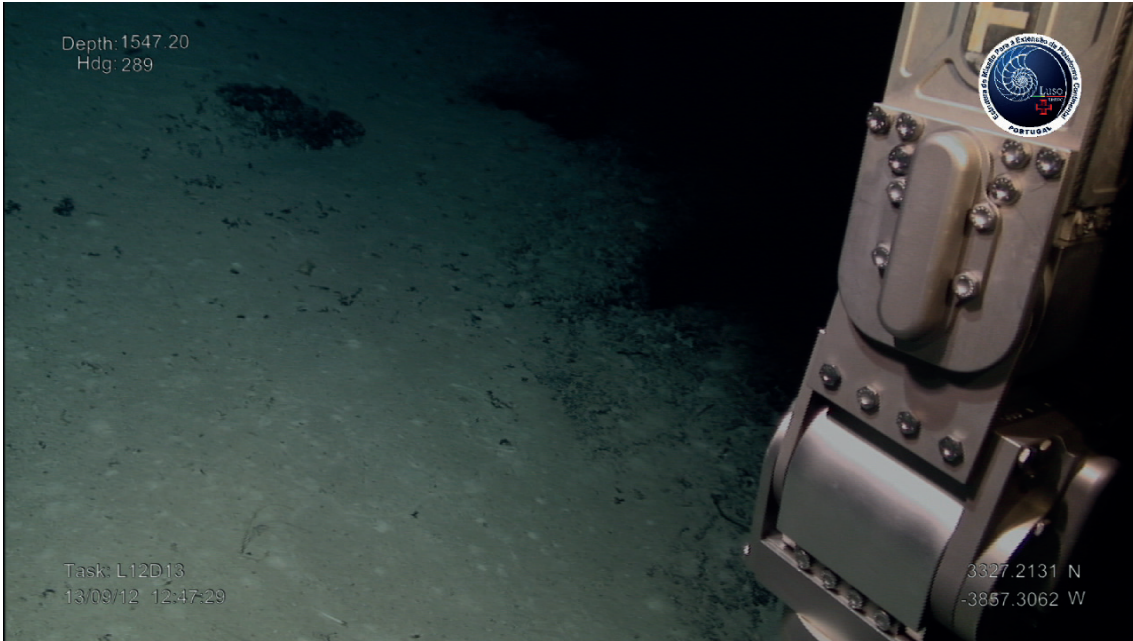
TIME (GPS)	LAT	LON	DEPTH (m)	HEADING	OBS.	Sampling
10:57:42	33° 27.147 N	38° 57.160 W	0		Start of dive D13	
10:58:40	33° 27.147 N	38° 57.160 W	0	139	ROV on water	
11:50:00	33° 27.214 N	38° 57.2163 W	689	71	jellyfish (cnidaria)	
12:10:35	33° 27.1975 N	38° 57.2444 W	1109	148	pyrossoma(FIG_1)	
12:13:50	33° 27.1975 N	38° 57.2444 W	1209	147	some cnidaria	
12:27:00	33° 27.2200 N	38° 57.2752W	1545	149	anguiliforme	
12:28:50	33° 27.2253 N	38° 57.2752 W	1546	273	rov on the ground; 2 shrimp; 2fish;(FIG_2)	
12:26:00			1547	147	Rov arrival at the bottom. All the sea bottom is covered by whitish sediment. Not a single rock outcrop.	
12:31:00			1544	271	Heterogeneously dispersed areas of a darker sediment (sediment crusts?)	
12:32:19	33° 27. 2340 N	38° 57.2845 W	1546	269	shark(FIG_4); 2fish(FIG_3);	
12:35:00			1549	261	Detailed images of the darker stuff materials - it seems that are sediment crust similar to sample L12D12R1 collected in the last ROV dive.	
12:35:24	33° 27.2187 N	38° 57.2970 W	1548	269	Sticopathes(FIG_5); small fish;	
12:37:00	33° 27.2140 N	38° 57.3057 W	1549	262	Sticopathes; porifera(FIG_7); coral(sea pen)(FIG_6); polichaeta (tube worm)(FIG_8)(FIG_10)	
12:38:00			1548	293	good images of tthe contact sediment / crusts	
12:42:00			1548	276	T4 tries to break the rock; looks like carbonate material	
12:46:00	33° 27.2131 N	38° 57.3062 W	1547	287	Big black sea urchin(FIG_11);small brown fish(FIG_12;FIG_13;FIG_14);green porifera(FIG_15);white porifera(FIG_16); brittle star(ofiura)(FIG_16);	
12:48:00			1545	280	The volcanics are outcropping - pillows and small lava tubes - Sediment between them. Rounded in shape and some with buds on the surface. Some fractured. Visible intercalation of lava tubes and pillows.	
12:50:00	33° 27.2147 N	38° 57.3070 W	1546	262	ROV stopped to collect a pillow sample. A bud was broken but fallen on the bottom. Trying another outcrop to the left. Tube worm(polchaeta); yellow porifera(FIG_18); white porifera(FIG_20); coral; sample of rock;	L12D13R01

TIME (GPS)	LAT	LON	DEPTH (m)	HEADING	OBS.	Sampling
13:04:02	33° 27.2098 N	38° 57.3177 W	1545	276	White porifera(FIG_21);2 shrimp; brittle star(FIG_20);sample of rock; tube worm (poichaeta)	L12D13R02
13:05:00			1547	258	Big plan and very good images of lava tubes and pillows.	
13:08:00			1546	250	sample on the rox box. Trying now to collect the rest of the bud.	
13:09:00	33° 27.2065 N	38° 57.3190 W	1546	250	Collecting the piece of the pillow bud R01 that has fallen	L12D13R01
13:15:40	33° 27.2088 N	38° 57.3214 W	1545	262	tube worm (polichaeta)(FIG_22) shrimp (crustacea); coral(FIG_23)	
13:15:00			1545	260	Using the fixed arm we are going to try to sample a top of a pillow, which constitutes a larger and better sample for chemical analysis. But no success.	
13:21:00			1546	240	The first piece of the bud (observation 12.58) was collected from the bottom. All the three pieces came from the same pillow bud.	
13:27:00			1544	252	leaving the sampled area - irregular pillows having a lot of buds in the surface; some small lava tubes. Sedimente (20-30%) between the lavas.	
13:28:00	33° 27.2065 N	38° 57.3223 W	1543	252	rocks with porifera(FIG_24)(FIG_25); tube worm ; shark; sticopathes (red), coral	
13:31:00			1530	252	There is a possibility that the lava tubes dominate - what we have been called pillows could correspond to the termination of the lava tubes.	
13:32:00			1531	260	very very good images of lava tubes, forming a small haystack. Massive lavas in aspect.	
13:32:18	33° 27.2040 N	38° 57.3186 W	1542	282	white and yellw gorgonia(FIG_26), sticopathes; porifera; tube worm(polichaeta); corals; white porifera(FIG_27);	
13:39:00			1531	0	detailed images of lava tubes.	
13:40:00					Clear images showing the lava tubes forming small haystacks	
13:42:53	33° 27.2073 N	38° 57.3372 W	1531	270	Gorgonia(FIG_28); porifera; shrimp; black fish(FIG_30); sea pen coral(FIG_30;FIG_31;FIG_32); hexactinelidae; sticopathes;pink coral(FIG_32) ;	
13:51:00			1532	286	more lava tubes	
13:54:00			1533	266	Trying to sample a lava tube bud.	
14:01:00			1532	285	very good image of small lava tubes	
14:01:00			1530	276	Still on the same area, but the rocks are very massive and, until now, both arms have been unsuccesfully in sampling. Very hard volcanics.	
14:03:06	33° 27.2030 N	38° 57.3385 W	1530	273	small fish; gorgonia; sea pen coral pink; jellyfish (cnidaria)(FIG_33); anguiliforme(FIG_35); coral	
14:06:57	33° 27.2019 N	38° 57.3276 W	1531	256	gorgonia; anemone; white porifera; coral(FIG_36)(FIG_37)	
14:15:00			1531	286	Flying following azimute 285. More plan, the relief, and again all sediment and sediment crusts.	
14:17:00	33° 27.1975 N	38° 57.3386 W	1530	263	big white sponge; branched coral	

TIME (GPS)	LAT	LON	DEPTH (m)	HEADING	OBS.	Sampling
14:17:00			1532	221	More small lava tubes mixed with sediment (50 / 50%).	
14:23:05	33° 27.1985 N	38° 57.3393 W	1531	261	branched pink coral(FIG_39); big white porifera(FIG_38); gorgonia;	
14:26:30	33° 27.1935 N	38° 57.3388 W	1531	235	yellow porifera, white porifera; (FIG_40)	
14:30:23	33° 27.1958 N	-3857.3380 W	1528 m	239	mollusca(FIG_42) sticopathes; sea anemone; tunicata(FIG_40)(FIG_41)	
14:33:13	33°27.1958 N	-3857.3438 W	1522	235	sea urchin(FIG_43)(FIG_44); fish; white porifera; red shrimp; gorgonia;	
14:34:00			1521	232	going up (steep slope) on a haystack made by big lava tubes - very massive a partially covered by sediment.	
14:40:44	33° 27.1837 N	38° 57.3381 W	1519	251	Branched coral; lobular porifera(FIG_46)(FIG_45); Fish; sea anemone(FIG_47)	
14:45:00			1519	257	good image of the steep slope	
14:50:50	33° 27.1885 N	38° 57.3457 W	1524	253	rocks with corals(FIG_48);sea anemones; white gorgonia , several porifera(FIG_49)(FIG_50)	
14:50:00			1524	225	The lava tubes are now more abundant and having higher dimensions. Some rounded pillows.	
14:59:00			1521	155	Irregular forms of pillows + lava tubes. Stop for sampling a termination of a small lava tube. No success. Outcrop forming a scarp relief.	
15:02:16	33° 27.1849 N	38° 57.3476 W	1520	173	Several poriferas with corals(FIG_51); sample of rock	L12D13R03
15:06:57	33° 27.1731 N	38° 57.3531 W	1513	156	fish(FIG_52)	
15:08:00			1509	166	more irregular lava tubes.	
15:10:00			1500	151	pink coral(FIG_53)	
15:14:00			1498	197	pink coral(FIG_54)	
15:16:00	33° 27.1698 N	38° 57.3318 W	1499	200	Another piece of the pillow bud, bigger than the others and liver shape.	L12D13R04
15:18:00	33° 27.167 N	38° 57.3368 W	1500	205	In the area of R# we are going to do a suction of the sediment and dead coral? It seems that the suction didn't work.	
15:26:01	33° 27.1670 N	38° 57.3368 W	1501	203	corer sample	L12D13C01
15:31:35	33° 27.1704 N	38° 57.3343 W	1501	179	sea urchin; coral(FIG_55); poriferas (hexactinellidae)(FIG_56); gorgonia;	
15:35:33	33° 27.0708 N	38° 57.3345 W	1500	183	sea anemone	
15:36:00			1499	138	pilled lava tubes, irregularly distributed.	
15:36:00	33° 27.1687 N	38° 57.3291 W	1497	167	vesel Sponge(FIG_58), crustacea	

TIME (GPS)	LAT	LON	DEPTH (m)	HEADING	OBS.	Sampling
15:39:00			1488	223	top of the haystack. Massive lava tubes and tabular lavas too (sheet flow).	
15:40:15	33° 27.1713 N	38° 57.3280 W	1487	175	corals and poriferas(FIG_57), sticopathes; shrimp; sponges(FIG_59)	
15:50:00	33° 27.1659 N	38° 57.3152 W	1489	210	Other sample collected at the top of the haystack - fragment of a small lava tube. Coral attached; rock with sticopathes; sea urchin;	L12D13R05
15:55:48	33° 27.1748 N	38° 57.3165 W	1493	85	Niskin	L12D13N1
16:20:28	33° 27.1395 N	38° 57.3288 W	597	87	Niskin	L12D13N2
16:28:24	33° 27.2004 N	38° 57.3395 W	148	123	Niskin (failed)	
16:30:00	33° 27.2023 N	38° 57.3457 W	102	123	Niskin	L12D13N3
16:36:00			0		end of dive	
			0		ROV on deck	

a



b



c



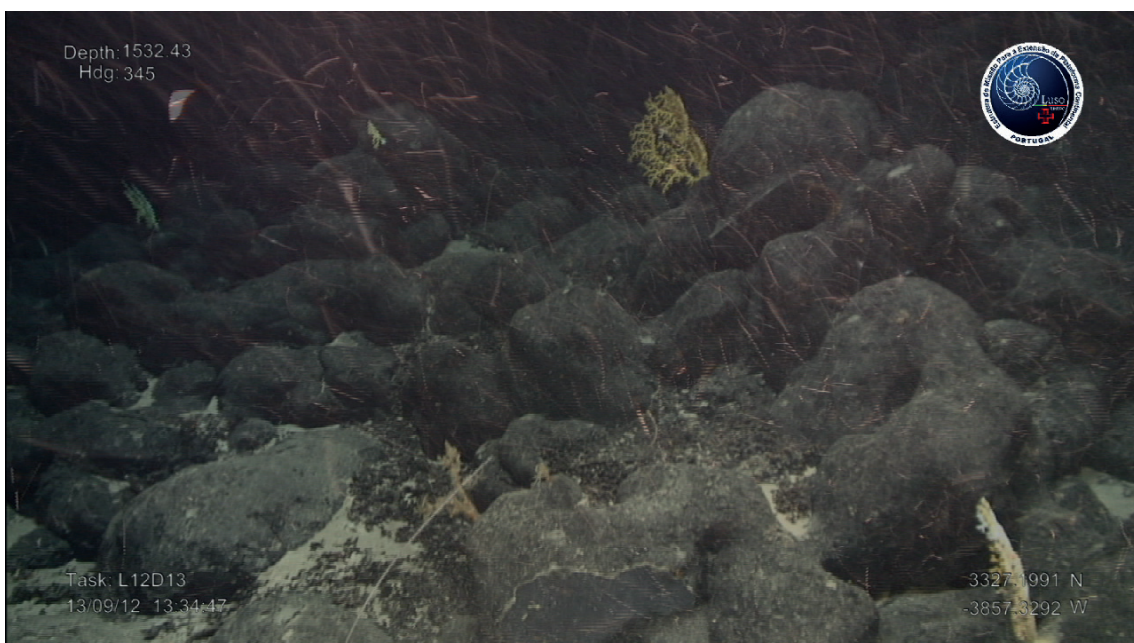
d



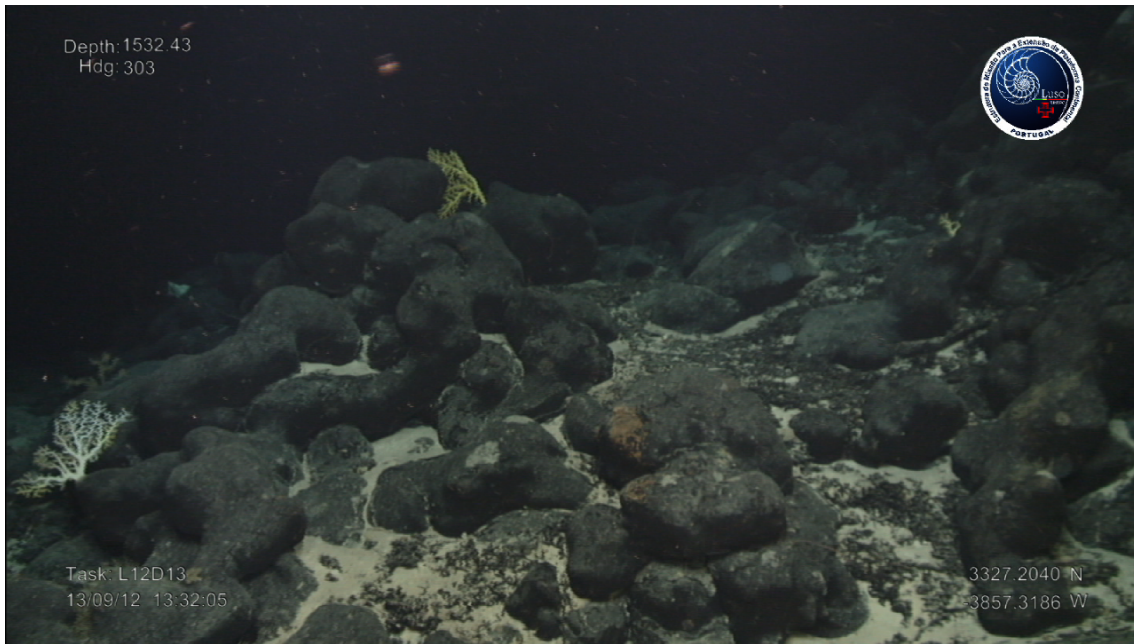
e



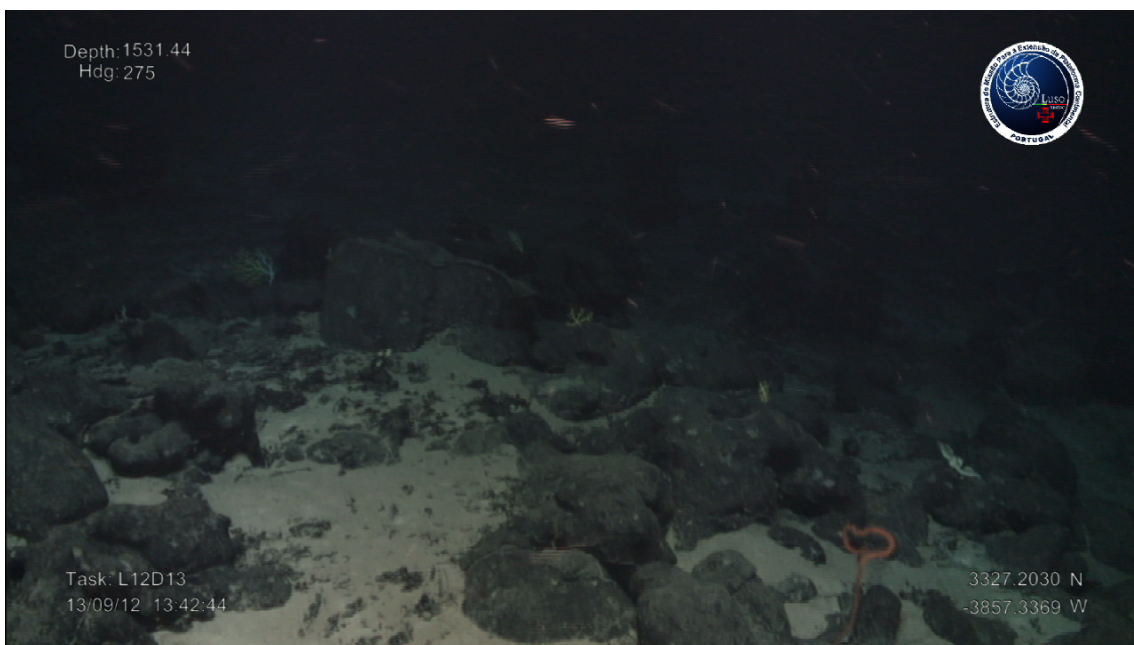
f



g



h



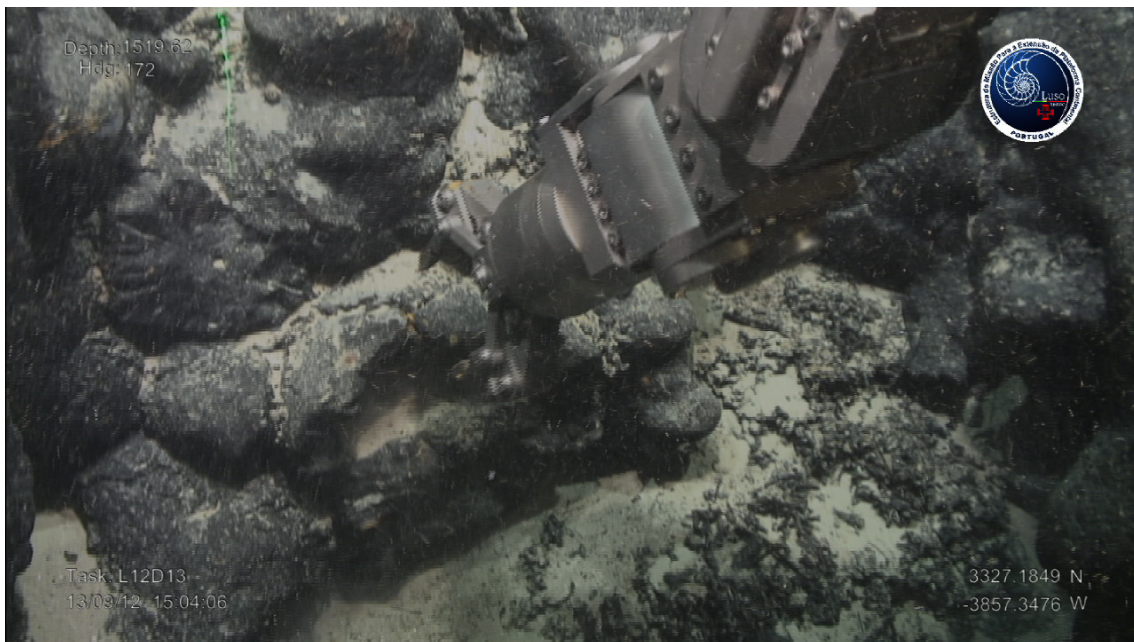
i



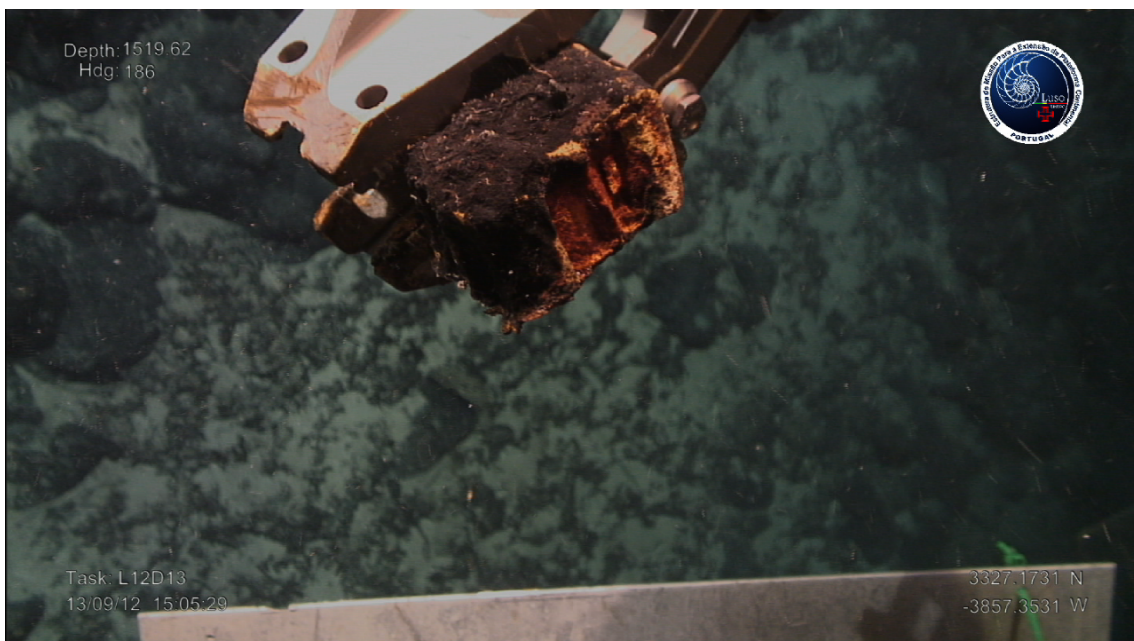
j



k



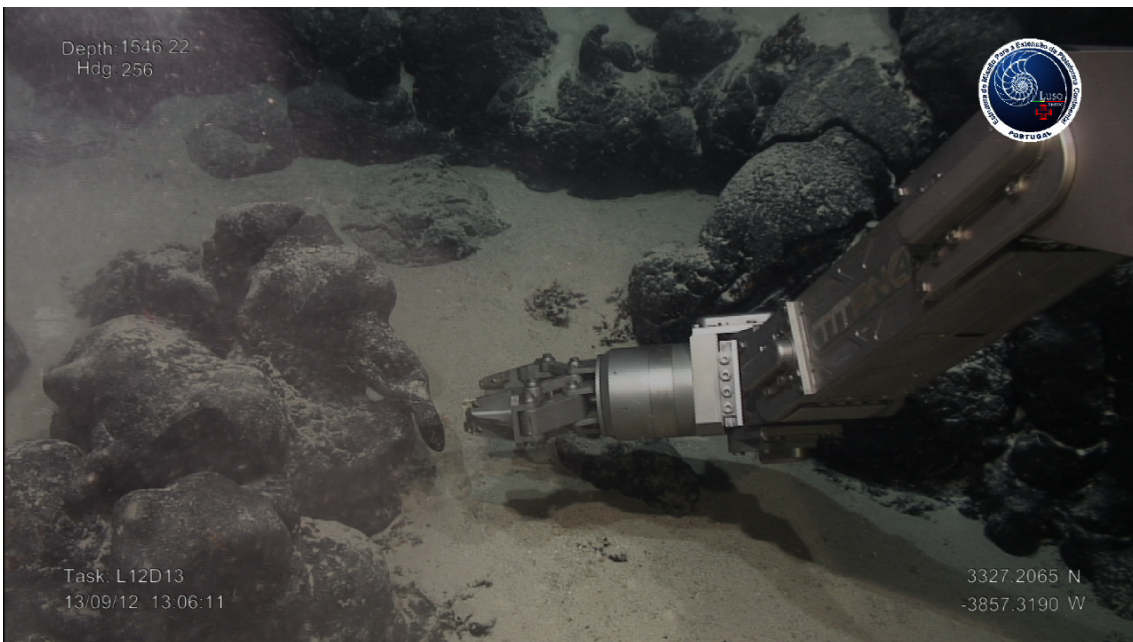
l



m



n



o



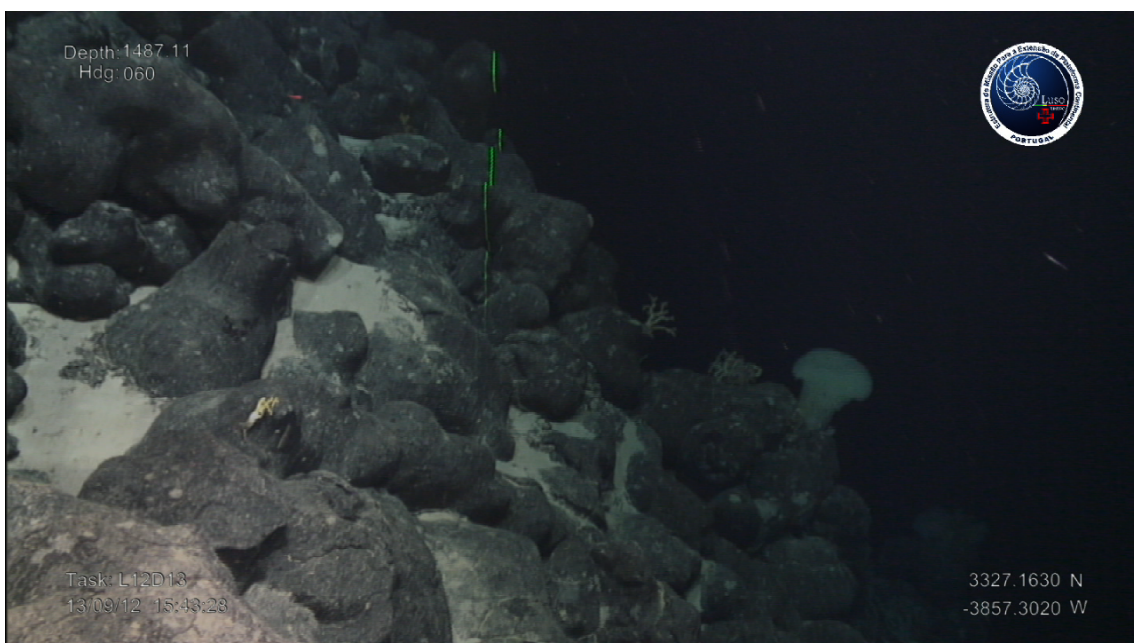
p



q



r



S



Basalt L12D13R01

LAT	LON	Depth	Date
33° 27.2059 N	38° 57.3267 W	1546	13.09.12



Morphology	Lava tube bud	Mass	300 gr
Age (0-4)	2	Size	14 x 3 x 4 cm

External Surface

Glass	Fe-OH	Mn-OH	Palagonite
		100 %	

Phenocrysts

	Oxide	Olivine	Plag	Cpx
Y/N	N	N	N	N
%				
Size				
Shape				

Matrix

Glassy	Cryptoxl	Massive	% area
		Y	

Vesicles

%	Size	Shape	Distribution
5 %	1 – 2 mm	rounded	random

Fractures

Y/N	%	Precipitates
Y	2%	Fe-OH

Remarks/Alteration

Beneath the Mn-OH cover there is palagonite (oxidized) with interbedded millimetric sized pristine glass veins. Phenocrysts are absent, however micro-phenocrysts of plagioclase are abundant reaching up to 2 mm, with subhedral to euhedral shape. Olivine as micro-phenocryst is rare and altered.

Basalt L12D13R02

LAT	LON	Depth	Date
33° 27.2065 N	38° 57.3190 W	1546	13.09.12



Morphology	Lava tube bud	Mass	150 gr
Age (0-4)	2	Size	4 x 3 x 4 cm

External Surface

Glass	Fe-OH	Mn-OH	Palagonite
		100 %	

Phenocrysts

	Oxide	Olivine	Plag	Cpx
Y/N	N	N	N	N
%				
Size				
Shape				

Matrix

Glassy	Cryptoxtl	Massive	% area
		Y	

Vesicles

%	Size	Shape	Distribution
3 - 5 %	1 mm	rounded	random

Fractures

Y/N	%	Precipitates
Y	2%	Fe-OH

Remarks/Alteration

Beneath the Mn-OH cover there is a palagonite (oxidized) with Fe-OH. Phenocrysts are absent, however micro-phenocrysts of plagioclase are abundant reaching up to 2 mm, with subhedral to euhedral shape. Olivine as micro-phenocryst is less rare than R01 and altered.

Basalt L12D13R03

LAT	LON	Depth	Date
33° 27.1731 N	38° 57.3531 W	1519	13.09.12



Morphology	Pillow lava rim	Mass	300 gr
Age (0-4)	2	Size	6 x 6 x 3 cm

External Surface

Glass	Fe-OH	Mn-OH	Palagonite
		100 %	

Phenocrysts

	Oxide	Olivine	Plag	Cpx
Y/N	N	N	Y	N
%			1 %	
Size			3 mm	
Shape			euohedral	

Matrix

Glassy	Cryptoxl	Massive	% area
		Y	

Vesicles

%	Size	Shape	Distribution
5 %	1 mm	rounded	random

Fractures

Y/N	%	Precipitates
Y	2%	Fe-OH

Remarks/Alteration

Beneath the Mn-OH cover there is palagonite (oxidized) with Fe-OH. Phenocrysts are absent, however micro-phenocrysts of plagioclase are abundant reaching up to 2 mm, with subhedral to euohedral shape. Olivine as micro-phenocryst is less rare than R01, and is altered.

Basalt L12D13R04

LAT	LON	Depth	Date
33°27.1698 N	38° 57.3318 W	1499	13.09.12



Morphology	Lava tube bud	Mass	2 kg
Age (0-4)	2	Size	16 x 8 x 6 cm

External Surface

Glass	Fe-OH	Mn-OH	Palagonite
		100 %	

Phenocrysts

	Oxide	Olivine	Plag	Cpx
Y/N	N	N	Y	N
%			1 %	
Size			2 mm	
Shape			euhedral	

Matrix

Glassy	Cryptoxl	Massive	% area
		Y	

Vesicles

%	Size	Shape	Distribution
5 - 8 %	1 mm	rounded	random

Fractures

Y/N	%	Precipitates
Y	5%	Fe-OH

Remarks/Alteration

Beneath the Mn-OH cover there is palagonite (oxidized) with Fe-OH. Phenocrysts are absent, however micro-phenocrysts of plagioclase are abundant reaching up to 2 mm, with subhedral to euhedral shape. Olivine as micro-phenocryst is less rare than R01 and altered.

Basalt L12D13R05

LAT	LON	Depth	Date
33° 27.1659 N	38° 57.3152	1489	13.09.12



Morphology	Lava tube bud	Mass	3 kg
Age (0-4)	2	Size	15 x 12 x 9 cm

External Surface

Glass	Fe-OH	Mn-OH	Palagonite
10		80 %	10

Phenocrysts

	Oxide	Olivine	Plag	Cpx
Y/N	N	N	Y	N
%			1 %	
Size			2 mm	
Shape			euhedral	

Matrix

Glassy	Cryptoxl	Massive	% area
		Y	

Vesicles

%	Size	Shape	Distribution
< 5 %	1 mm	rounded	Rim and core of the lava

Fractures

Y/N	%	Precipitates
Y	5%	Fe-OH, whitish material (carbonate?)

Remarks/Alteration

Beneath the Mn-OH cover there is palagonite (oxidized) with Fe-OH. Phenocrysts are absent, however micro-phenocrysts of plagioclase are abundant reaching up to 2 mm, with subhedral to euhedral shape. Olivine as micro-phenocryst is less rare than R01 and altered. Concentric layering, visible on the rock surfaces that are parallel to the fractures. On the lava's core a 2 x 1 cm hole is filled with Fe-OH, palagonite, sulphates (gypsum?), glass, carbonate (?).